Evolutionary divergence of enzymatic mechanisms for posttranslational polyglycylation.

Krzysztof Rogowski, François Juge, Juliette van Dijk, Dorota Wloga, Jean-Marc Strub, Nicolette Levilliers, Daniel Thomas, Marie-Hélène Bré, Alain van Dorsselaer, Jacek Gaertig, et al.

Evolutionary divergence of enzymatic mechanisms for posttranslational polyglycylation

Krzysztof Rogowski[1], François Juge[2], Juliette van Dijk[1], Dorota Wloga[3], Jean-Marc Strub[4], Nicolette Levilliers[5], Daniel Thomas[6], Marie-Hélène Bré[5], Alain Van Dorsselaer[4], Jacek Gaertig[3] and Carsten Janke[1#]

[1]CRBM, CNRS, Université Montpellier 2 and 1, 34293 Montpellier, France;

[2]IGMM, CNRS, Université Montpellier 2, 34293 Montpellier, France;

[3]Department of Cellular Biology, University of Georgia, Athens 30602-2607 GA, USA;

[4]LSMBO, Université Louis Pasteur, CNRS, 67087 Strasbourg, France;

[5]Laboratoire de Biologie Cellulaire 4, CNRS, Université Paris-Sud 11, 91405 Orsay, France

[6]Interactions Cellulaires et Moléculaires, CNRS, Université de Rennes 1, 35042 Rennes, France

#corresponding author: Carsten Janke

CRBM, CNRS, 1919 route de Mende, 34293 Montpellier, France

Telephone: +33 4 67613335

Fax: +33 4 67521559

Email: carsten.janke@crbm.cnrs.fr

Keywords: Tubulin, microtubules, glycylation, axoneme, flagella

Summary

Polyglycylation is a posttranslational polymodification that generates glycine side chains on proteins. It was discovered more than ten years ago on tubulin, and is prominent in cilia and flagella. Yet the enzymes that catalyze tubulin polyglycylation have remained unknown. Here we describe the identification of a family of evolutionary conserved glycine ligases that modify tubulin. In mammals, two distinct enzyme types catalyze the initiation and elongation steps of polyglycylation, whereas the *Drosophila* enzymes are bifunctional. Depletion of a polyglycylase in *Drosophila* using RNA interference results in adult flies with strongly decreased polyglycylation levels and male sterility associated with defects in sperm individualization and axonemal maintenance. A more severe RNAi depletion is lethal at early developmental stages, indicating that protein glycylation is essential. Together with the observation that multiple proteins are polyglycylated, our functional data point towards a general role of polyglycylation in protein functions.

Introduction

Polyglycylation is a posttranslational modification that generates side chains of glycine on the γ-carboxyl groups of specific glutamate residues of target proteins (Bré et al., 1998; Vinh et al., 1999). Similarly to polyglutamylation (Eddé et al., 1990), this posttranslational modification was discovered on tubulin, where it occurs within the carboxy-terminal tail domains (Redeker et al., 1994). While polyglutamylation was observed on many different types of microtubules (MTs), polyglycylation is particularly prominent in cilia and flagella and is mostly found in cells that possess these organelles (Bré et al., 1996; Levilliers et al., 1995).

Functional experiments on tubulin glycylation were difficult to perform since the modifying enzymes were unknown. Initial insights into the potential function of polyglycylation were obtained using modification-specific antibodies. For example, anti-glycylation antibodies affected axoneme beating *in vitro*, suggesting that tubulin polyglycylation could regulate ciliary dynein (Bré et al., 1996). In *Tetrahymena*, the elimination of the major glycylation sites on β-tubulin was lethal or led to severe axonemal defects, including short axoneme size, absence of the central pair MTs, and incomplete outer doublet MTs (Redeker et al., 2005; Thazhath et al., 2002; Xia et al., 2000). Thus, tubulin glycylation could be an important regulator of both the assembly and functions of axonemal MTs. The recent observations that non-tubulin proteins are also substrates of polyglycylation (Ikegami et al., 2008; Lalle et al., 2006; Xie et al., 2007) indicate that glycylation is a posttranslational modification of general importance.

Here we describe the discovery of a group of enzymes that catalyze tubulin glycylation and show that some of these enzymes have non-tubulin substrates. We

demonstrate that glycylases are members of the tubulin tyrosine ligase-like (TTLL) family, which already contains three types of known amino acid ligases, the tubulin tyrosine ligase (TTL; Ersfeld et al., 1993), polyglutamylases (Janke et al., 2005; van Dijk et al., 2007; Wloga et al., 2008) and an enzyme that ligates glycine to nucleosome assembly protein 1 (NAP1; Ikegami et al., 2008). We show that in mouse, TTLL3 and TTLL8 proteins are initiating glycylases with different substrate specificities, whereas TTLL10 is the elongating polyglycylase. Cooperation of these two types of enzymes generates polyglycine side chains in mammals, whereas in *Drosophila*, bifunctional enzymes catalyze both reactions. We also demonstrate that the previously reported absence of long glycine side chains on human sperm tubulin (Bré et al., 1996) is caused by two inactivating amino acid substitutions in human TTLL10. Finally, we show by RNA interference (RNAi) that depletion of one of the two glycylases in *Drosophila* leads to strong reduction in polyglycylation, which causes defects in sperm maturation and results in male sterility. Moreover, expression of interfering RNA under a stronger promoter is lethal in early developmental stages. This suggests that polyglycylation is important for whole-organism development in *Drosophila*. The identification of new substrates of glycylation indicates that this modification could have a broad range of functions.

Results

Identification of murine polyglycylases

Our study was initiated with the hypothesis that tubulin glycylases, like two other types of tubulin amino acid ligases, TTL (Ersfeld et al., 1993) and polyglutamylases (Janke et al., 2005; van Dijk et al., 2007), are members of the TTLL protein family.

Within the mammalian TTLL family, TTLL3, 8, 10 and 12 remained uncharacterized. According to phylogenetic studies, the *TTLL12* gene is present in species that appear to lack glycylation (Janke et al., 2005; Schneider et al., 1997), and murine TTLL12 has no glycylation activity *in vivo* and *in vitro* (KR, unpublished observations). In contrast, the presence of orthologs of *TTLL3*, *8* and *10* in genomes of diverse species (Janke et al., 2005) correlates with the known presence of tubulin glycylation, and a recent study showed that one of these three genes, *TTLL10*, encodes a glycylase for NAPs (Ikegami et al., 2008).

To test whether mouse TTLL3, 8 and 10 have a tubulin glycylase activity, we expressed the respective cDNAs (van Dijk et al., 2007) in HEK293 cells and tested the cell extracts in an *in vitro* MT glycylation assay. To distinguish between two possible types of activities, initiation (addition of the first glycine to a γ-carboxyl group of the target glutamate residue) and elongation of glycine side chains, we used substrates differing in the levels of tubulin glycylation: MTs polymerized from brain tubulin (that lack detectable glycylation) and strongly glycylated MTs of ciliary axonemes of *Tetrahymena thermophila*. Both, TTLL3 and 8 promoted incorporation of [^{3}H]-glycine into brain MTs, but had very low activity on axonemal MTs. In contrast, TTLL10 was almost inactive on brain MTs, but promoted efficient [^{3}H]-glycine incorporation into axonemal MTs (Fig. 1A). These observations suggest that TTLL3 and 8 are initiating glycylases, whereas TTLL10 is an elongating glycylase (polyglycylase) for tubulin. A similar functional specialization has been previously observed among polyglutamylases (van Dijk et al., 2007; Wloga et al., 2008).

We also examined the selectivity of the enzymes for α- and β-tubulin. TTLL3 and 8 modified both, α- and β-tubulin of brain MTs, with TTLL8 showing preference for α-

tubulin (Fig. 1A). For TTLL10, which modified only axonemal MTs, two-dimensional electrophoresis was used to separate axonemal α- and β-tubulin. Using anti-α- or β-tubulin antibodies as well as TAP952 (an antibody that recognizes monoglycylated sites on tubulins; Bré et al., 1998) we found that both tubulin subunits of *Tetrahymena* axonemes are monoglycylated, and thus are potential substrates for the elongation reaction. However, TTLL10 incorporated [^{3}H]-glycine mainly into α-tubulin (Fig. 1B).

Next, we expressed TTLL3, 8 and 10 in U2OS cells and labeled the cells with antibodies that are specific to either mono- or polyglycylation: TAP952 and polyG (polyG specifically recognizes polyglycine chains; Duan and Gorovsky, 2002), respectively (Fig. 1C). Non-transfected U2OS cells show no reactivity with either of these two antibodies (arrowheads). After expression of TTLL3 or 8, we detected specific labeling of MTs with TAP952, but not with polyG. Thus, TTLL3 and 8 mediate initiation of glycine side chains on MTs *in vivo*, but not side chain elongation. In contrast, cells expressing TTLL10 alone showed no labeling with TAP952, but had a diffuse labeling with polyG that did not correspond to MTs. This suggests that TTLL10 adds polyglycine chains directly onto proteins that are not associated with MTs, while it cannot modify MTs without prior monoglycylation.

Two-step glycylation mechanism in mammals

To test whether the two types of mammalian glycylases can function in a cooperative manner to create long side chains on MTs, we co-overexpressed either TTLL3 or 8 together with TTLL10 in U2OS cells. In both cases, we observed a strong labeling of MTs with the polyG antibody (Fig. 2A). These results indicate that MTs

have acquired polyglycine side chains, which was not the case when TTLL3, 8 or TTLL10 were expressed alone (Fig. 1C).

On immunoblots, the monoglycylation-specific antibody TAP952 detected strong signals in the tubulin region upon expression of TTLL3 or 8 alone. Additional protein bands were labeled after TTLL8 expression, suggesting that TTLL8 can mediate glycylation of other non-tubulin proteins (Fig. 2B). TTLL3 increased glycylation of mostly β-tubulin in U2OS cells, while it promoted modification of both α- and β-tubulin in the *in vitro* assay (Fig. 2B, 1A). Thus, it appears that the substrate preferences of the glycylating enzymes change depending on additional factors. Neither TTLL3 nor TTLL8 alone generated polyG-reactive epitopes, indicating that they are indeed restricted to reactions that generate monoglycine side chains (Fig. 2B). In contrast, no TAP952 labeling was detected in extracts of cells expressing TTLL10. However, a strong polyG signal was induced on two distinct protein bands, one of them the size of α-tubulin (Fig. 2B). We demonstrate that the substrate in the tubulin region corresponds to NAPs. First, two-dimensional immunoblot analysis shows that the polyglycylated 50 kDa protein band superimposes with NAPs, but not with tubulins (Fig. 2C), and second, ectopically expressed NAP1-EYFP and NAP2-EYFP were strongly polyglycylated by TTLL10 (Fig. S1). This is in agreement with the results of Ikegami et al. (2008) and indicates that in contrast to tubulins, NAPs can be polyglycylated directly by TTLL10.

After co-expression of TTLL3 or 8 with TTLL10, no TAP952 labeling was detected, whereas several protein bands were labeled with the polyG antibody. Virtually all protein bands labeled with TAP952 after expression of TTLL3 or 8 alone became labeled with polyG when TTLL10 was co-expressed (Fig. 2B), suggesting that

following monoglycylation by TTLL3 or 8, TTLL10 elongates glycine side chains of all major substrates of the initiating enzymes. The efficiency of this process is illustrated by the reduction of monoglycylated epitopes below detectable levels. This further indicates that the substrate specificity of polyglycylation in mammals is predetermined by the specificity of the initiating glycylases rather than by the elongating enzyme, except for proteins that are directly modified by TTLL10, such as the NAPs.

Loss of elongating activity in humans

Human sperm axonemes, unlike sperm axonemes of several other mammalian species studied so far, have side chains limited to monoglycylation (Bré et al., 1996). We confirmed this by comparing the status of glycylation in protein extracts prepared from mouse, rhesus monkey and human sperm using the TAP952 and the polyG antibody (Fig. 3A). Several mouse and rhesus protein bands were strongly labeled with polyG, while only weak signals were detected with TAP952. In contrast, human sperm proteins were not labeled with polyG, but strongly with TAP952. No differences between the three species were found for the related tubulin modification, polyglutamylation (Fig. 3A, panel polyE).

To determine the molecular basis for the lack of elongated polyglycine chains in human sperm, we investigated the only known elongating glycylase in mammals, TTLL10. First, we confirmed the presence of a full-length mRNA by cloning TTLL10 from human testes cDNA. We then expressed human, mouse and rhesus TTLL10 in U2OS cells. The mouse and rhesus TTLL10 generated polyglycylation that could be specifically detected with polyG, whereas the human protein was inactive (Fig. 3B). Accordingly, when cell extracts from HEK293 cells overexpressing the respective

TTLL10 proteins were used for *in vitro* assays, only the mouse and rhesus, but not the human TTLL10 mediated incorporation of [^{3}H]-glycine into axonemal MTs (Fig. 3C). Domain-swapping experiments localized the inactivating mutations to the central region of human TTLL10, which corresponds to the highly conserved core TTL domain (Fig. S3, S4A, B; van Dijk et al., 2007). Within this domain, human and rhesus TTLL10 differ by 11 amino acids, out of which 4 are not evolutionarily conserved. Thus, we analyzed the remaining 7 amino acid changes by introducing them separately into the rhesus TTLL10. Two of these mutations led to a complete loss of polyglycylase activity (Fig. S3, S4C), suggesting that the corresponding amino acids are essential for activity. When these two mutations in human TTLL10 were both reverted to the conserved amino acids found in rhesus and mouse, the enzyme recovered polyglycylase activity (Fig. 3D, E). This was not the case if only one mutation was reverted. As neither of the two mutations has been found in the genomes of the great apes (not shown), it appears that humans are unique in having lost the polyglycylation activity of TTLL10. One of the two inactivating mutations (mut3) is polymorphic in the human population, leading to a high incidence (55.0% heterozygote and 16.7% homozygote) of TTLL10 alleles without mut3 in the sub-Saharan African population, whereas 91.7% of the European population are homozygote for the presence of mut3 (http://www.ncbi.nlm.nih.gov/SNP/snp_ref.cgi?rs=1320571). No polymorphism was found for mut5. To investigate if the mut3 polymorphism could affect the enzymatic activity of TTLL10, we compared polyglycylation of sperm proteins from two homozygote individuals either with or without mut3, but both bearing mut5 (Fig. S5A). The complete absence of polyglycylation on sperm proteins from both individuals

(Fig. S5B) confirmed that the presence of one of the two inactivating mutations is sufficient for the complete loss of enzymatic activity of human TTLL10 (Fig. S4C).

In conclusion, we show that the human elongating polyglycylase TTLL10 is functionally inactive due to two mutations, resulting in the absence of polyglycylation in sperm. Considering that all known amino acid ligases that modify tubulin are members of the TTLL family, and that all TTLLs are expressed in testes (Ersfeld et al., 1993; van Dijk et al., 2007), it is likely that TTLL10 is the only polyglycylating enzyme in mammals. Thus, humans could be a unique mammalian species that lacks protein polyglycylation.

Cancer-associated mutations inactivate the TTLL3 enzyme

In a recently published screen for putative cancer-associated genes, *TTLL3* obtained a relatively high score as a potential cancer gene (Sjöblom et al., 2006). It was striking that the two mutations identified in the screen were localized in the vicinity of the ATP-binding residue E662, which is essential for enzymatic activity in all TTLLs (Fig. 4A; van Dijk et al., 2007). To test the potential impact of these mutations, we introduced them separately into mouse TTLL3, which is identical to human TTLL3 in this region (Fig. 4A), and tested the enzymatic activity of the mutated enzymes. Each cancer-related mutation led to a complete loss of glycylase activity of TTLL3 *in vivo* and *in vitro* (Fig. 4B-D), suggesting that loss of monoglycylating activity could be related to cancer.

A divergent polyglycylation mechanism in Drosophila

In mammals, TTLL10 is the only enzyme able to elongate glycine side chains. However, in *Drosophila*, an organism with polyglycylated MTs (Bré et al., 1996), only

two orthologs of the TTLL3/8 group are present, whereas no *TTLL10* gene has been found (Janke et al., 2005). To establish the enzymatic mechanism that leads to the elongation of glycine side chains in the absence of TTLL10, we investigated the activity of the *Drosophila melanogaster* (dm) enzymes dmTTLL3A (CG11323) and dmTTLL3B (CG11201) in U2OS cells. Both enzymes induced monoglycylation on MTs (Fig. 5A, panel TAP952). Some cells expressing dmTTLL3B showed a restricted localization of this enzyme to the nucleus, and accordingly, only the nucleus was labeled with TAP952 in those cells (Fig. 5A, #). However, in contrast to the mammalian orthologs (Fig. 1C), dmTTLL3A also generated polyglycylated MTs as detected with polyG, while dmTTLL3B polyglycylated nuclear proteins, but not MTs (Fig. 5A, panel polyG). Immunoblots revealed that dmTTLL3A initiates and elongates glycine side chains on α- and β-tubulin, whereas dmTTLL3B initiates glycylation on number of proteins including α-tubulin, but functions as an elongating polyglycylase only for non-tubulin substrates (Fig. 5B). These polyglycylated substrates of yet unknown identity are likely to be responsible for the observed nuclear staining (Fig. 5A). Thus, *Drosophila* has a polyglycylation mechanism that utilizes bifunctional initiating/elongating polyglycylases.

dmTTLL3B is essential in Drosophila

Polyglycylation is particularly abundant in testes where it is associated with the axonemes of the sperm flagella (Bré et al., 1996; Bressac et al., 1995). In *Drosophila*, one of the polyglycylase genes, *dmTTLL3B*, is highly expressed in testes (Fig. S6), suggesting that dmTTLL3B is the major polyglycylase in this organ. Thus, we attempted to deplete dmTTLL3B by RNA interference (RNAi), using a transgenic fly carrying inverted repeats that correspond to *dmTTLL3B* under the control of *UAS*

sequences inducible by Gal4 (*UAS-IR-dmTTLL3B* transgene). Strikingly, 50% of the embryos carrying *UAS-IR-dmTTLL3B* and the ubiquitous *da-Gal4* driver ($dmTTLL3B^{da\text{-}RNAi}$) did not survive to adulthood (Fig. 6A).

RT-PCR analysis of adult $dmTTLL3B^{da\text{-}RNAi}$ flies demonstrated that *dmTTLL3B* inverted repeats were expressed and *dmTTLL3B* mRNA levels were strongly decreased. In contrast, mRNA levels of the closest homolog of this gene, *dmTTLL3A*, were unchanged (Fig. 6B), demonstrating the specificity of the *dmTTLL3B* RNAi. Immunoblots of whole-protein extracts showed a strong reduction of polyG-labeling on a range of protein bands in the $dmTTLL3B^{da\text{-}RNAi}$ flies (Fig. 6C), whereas polyglutamylation levels were slightly increased in males but not in females (Fig. 6C, panel GT335). These data provide strong evidence that the majority of the protein polyglycylation in *Drosophila* is catalyzed by dmTTLL3B. Almost all adult male $dmTTLL3B^{da\text{-}RNAi}$ flies were sterile, as only 2.4% were able to generate offspring (Fig. 6D), although with 20 times less progeny as compared to wild type. This suggests that polyglycylation is important for spermatogenesis.

The process of spermatogenesis in *Drosophila* can be divided into three major steps: (i) the generation of 64 haploid, interconnected spermatocytes from a stem cell, (ii) the formation of the axonemes and the condensation of the sperm nuclei in the still interconnected spermatids and (iii) the individualization that resolves the syncytial sperm bundle into 64 separate sperm cells. This last step is achieved by a group of synchronously moving individualization complexes that remove excess cytoplasm and place the membranes around each cell. To determine which of the three steps were affected in $dmTTLL3B^{da\text{-}RNAi}$ flies, we analyzed the testes by immunofluorescence and transmission electron microscopy (TEM). In immunofluorescence (Fig. 6E) of wild type

testes, the polyG antibody stained prominent bundles of fibers that correspond to the sperm tails. The actin staining visualized groups of regularly arranged individualization complexes, which were always associated with the polyG-reactive MT bundles, confirming that sperm polyglycylation appears at the onset of individualization (Bré et al., 1996; Bressac et al., 1995). In contrast, in *dmTTLL3B*$^{da\text{-}RNAi}$ testes, polyG staining was strongly reduced and actin cones were scattered along the tails, indicating a sperm individualization defect (Fabrizio et al., 1998). Moreover, we observe that the tips of the testes were often enlarged in *dmTTLL3B*$^{da\text{-}RNAi}$ male flies (Fig. 6E).

To better understand the observed defects we compared cross-sections of sperm cysts at different stages of maturity using TEM. In the preindividualization stage, sperm cysts of both control and *dmTTLL3B*$^{da\text{-}RNAi}$ flies appeared similar, as they contained the expected 64 sperm cells with an axoneme as well as a minor and a major mitochondrial derivate (Fig. 6F). Upon maturation, sperm cysts become more compact due to strongly reduced cytoplasmic ground substance. At this late stage, control cysts were highly organized as each axoneme was positioned in the close proximity of a major mitochondrial derivate (Fig. 6G, panel control). In contrast, most of the mature cysts from *dmTTLL3B*$^{da\text{-}RNAi}$ flies were lacking the axoneme structures, whereas the mitochondrial derivates were still present (Fig. 6G, panels *dmTTLL3B*$^{da\text{-}RNAi}$). In some cases, disorganized axonemes composed of singlet MTs were found. We also observed rare cases of disorganized cysts that still contained axonemes, but had reduced or absent mitochondria. Together our findings indicate that polyglycylation plays a role in individualization and is essential for the maintenance of the axoneme structure at later stages. However, it is not required for the early steps of *Drosophila* spermatogenesis, including the assembly of the axonemes.

Finally, we hypothesized that the initially observed partial lethality of the *dmTTLL3B*$^{da\text{-}RNAi}$ flies indicates an essential function of *dmTTLL3B* in *Drosophila*, and that the flies that reached adulthood survived due to the incomplete suppression of *dmTTLL3B* under the *da-Gal4* driver. To test this hypothesis, we increased the efficiency of the RNAi by introducing the *UAS-Dcr-2* transgene (Dietzl et al., 2007) into the *dmTTLL3B*$^{da\text{-}RNAi}$ flies. Strikingly, we observed 100% lethality at the larval stage. This phenotype is not due to side effects of the *UAS-Dcr-2* transgene (Dietzl et al., 2007), since the expression of *UAS-IR-dmTTLL3B* under the control of the very strong and ubiquitous *Act5C-Gal4* driver also led to 100% lethality (not shown). Thus, in addition to an important role in spermatogenesis, dmTTLL3B-mediated polyglycylation could be essential for *Drosophila* development.

Identification of potential new substrates of glycylation

The observation that mouse TTLL8 as well as *Drosophila* TTLL3B glycylate a range of non-tubulin proteins (Fig. 2B, 5B, 6C) raised the possibility that glycylation is a posttranslational modification with a broad range of substrates. Following the observation that the two most prominent substrates of polyglutamylation, tubulins (Eddé et al., 1990) and NAPs (Regnard et al., 2000), are also modified by polyglycylation (Redeker et al., 1994; Ikegami et al., 2008), we hypothesized that additional substrates of glycylation are among the previously identified substrates of polyglutamylation (van Dijk et al., 2008). We expressed 12 potential substrates of polyglutamylation together with either TTLL8 or an enzymatically inactive (dead) version of TTLL8 in HEK293 cells. Five proteins (ANP32A, ANP32B, SET, RanGAP and nucleolin) were found to be glycylated in the presence of active, but not inactive TTLL8 (Fig. 7). Seven other proteins tested (NF45, B23, GRP78, NASP, RNP-K, NCT,

EB1, data not shown) were not modified. To uncover additional substrates by a more direct approach, we separated proteins from fly testes using two-dimensional electrophoresis and analyzed polyG reactive proteins by mass spectrometry. We selected six of the identified proteins (Table S1; see supplementary information for more details) and co-overexpressed them with active or inactive TTLL8 in HEK293 cells. Among these proteins, troponin T was found to be specifically glycylated by ectopic TTLL8 (Fig. 7). The identification of a range of potential substrates of glycylation suggests that this modification could regulate the function of many proteins. Thus, the lack of glycylation of several proteins, and not only tubulin, could have contributed to the defects observed in the dmTTLL3B depleted flies.

Discussion

Polyglycylation was first described as a polymodification that generates glycine side chains of variable length on α- and β-tubulins (Redeker et al., 1994). Similarly to polyglutamylation, it targets the C-terminal tails of tubulins, which are the major interaction sites for MT-associated proteins and molecular motors (Nogales, 2000). Thus, polyglycylation could be an important regulator of MT functions.

We have identified a group of enzymes that mediate the generation of glycine side chains on proteins. The glycylating enzymes are members of the TTLL family, which also contains other enzymes that catalyze amino acid ligations: tubulin tyrosine ligase (Ersfeld et al., 1993) and diverse polyglutamylases (Janke et al., 2005; van Dijk et al., 2007; Wloga et al., 2008). Initiation and elongation of the glycine side chains are catalyzed by separate glycylases in mammals. Two initiating enzymes, TTLL3 and TTLL8, both generate monoglycylation on tubulin, whereas only TTLL8 modifies additional proteins. In agreement with our results, TTLL3 proteins in the ciliate

Tetrahymena and in zebrafish are also initiating tubulin glycylases (Wloga et al., 2009). The subsequent elongation of glycine side chains in mammals is catalyzed by the elongating polyglycylase TTLL10.

The discovery of a strict two-step mechanism for MT polyglycylation in vertebrates raised two questions related to previous descriptions of polyglycylation patterns in different organisms. First, elongated glycine side chains are completely absent in human sperm tubulin (Bré et al., 1996). We show that this phenotype is directly related to human TTLL10, which lacks enzymatic activity due to two point mutations in the conserved core TTL domain. It is striking that these mutations appear to be unique to human TTLL10, which suggests that the loss of polyglycylation was an event important for human evolution. Furthermore, the existence of a species devoid of polyglycylation suggests that the "poly" character of glycylation is not essential for protein functions, and that the functions of glycylation could be efficiently fulfilled by monoglycylation, which is present in all cilia in mammals (Dossou et al., 2007). Another surprising observation was that *Drosophila*, an organism with reported polyglycine side chains on tubulin (Bré et al., 1996), has no homologs of TTLL10. We show that in *Drosophila*, glycylases from the TTLL3/8 group act as bifunctional enzymes that are able to catalyze both, initiation and elongation of glycine side chains, explaining why polyglycine side chains are present despite the absence of a TTLL10 ortholog. The two distinct glycylation mechanisms in mammals and *Drosophila* correlate with the previously described order of appearance of polyglycylation during sperm maturation. In mouse, polyglycine side chain elongation is delayed, appearing only after initial monoglycylation (Kann et al., 1998), whereas in *Drosophila*, mono- and polyglycylation occur simultaneously (Bré et al., 1996).

In *Drosophila* the depletion of dmTTLL3B induced a significant decrease in glycylation, accompanied by decreased viability and an almost complete sterility of the surviving males. Detailed analysis of the *dmTTLL3B*$^{da\text{-}RNAi}$ flies revealed that the lack of dmTTLL3B affects late stages of spermatogenesis. This coincides with the timing of appearance of glycylation in *Drosophila* sperm development (Bressac et al., 1995). We observed that although axonemes were assembled, they become unstable and disassemble in final stages of spermatogenesis. The disassembly of the axonemes is likely to proceed through a stage in which MT doublets are reduced to singlets, followed by the complete disappearance of all MT structures. Thus, one of the roles of glycylation in spermatogenesis appears to be the maintenance of the axonemal structure, whereas the modification is not required for the assembly.

Due to their sensory role in cells, cilia are centers of signal transduction pathways involved in embryonic development and tissue homeostasis in adults. Therefore, defects in cilia can be related to cancer (Mans et al., 2008; Michaud and Yoder, 2006). Our finding that two cancer-related mutations in TTLL3 (identified by Sjöblom et al. 2006) both completely inactivate this enzyme, suggests that the lack of TTLL3 activity could affect cilia, which in turn could contribute to cancer progression.

The complexity of signals generated by polyglutamylation and polyglycylation on MTs could allow for different modes of regulation. Besides the possibility that both polymodifications generate signals for different target proteins, glycylation could also function as a counter-regulator of polyglutamylation, since both modifications compete for similar modification sites on tubulin (Redeker et al., 2005). In agreement with this hypothesis, we show that tubulin polyglutamylation increases upon depletion of polyglycylation. Such a function could be sufficiently fulfilled by monoglycylation,

which would help explaining the apparent lack of phenotypes related to the loss of elongated glycine side chain in humans.

Most of the past work on glycylation has been focussed on the role of this modification in MT functions; however, several recent studies have shown that other proteins are substrates of glycylation (Ikegami et al., 2008; Lalle et al., 2006; Xie et al., 2007). Together with our results, this opens the possibility that glycylation targets a broad range of substrates.

To conclude, we have identified a new group of tubulin modifying enzymes and two evolutionarily divergent mechanisms for glycyl side chain initiation and elongation. Functional studies in *Drosophila* show that glycylation is important for sperm maturation, and that it might also be essential in early developmental stages in flies. Finally, the discovery that several important proteins could undergo glycylation raises the possibility that this modification acts as a general regulator of cellular functions.

Experimental procedures

Cloning and mutagenesis

Mouse *TTLL3*, *8* and *10* have been identified and cloned before (van Dijk et al., 2007). The rhesus monkey (*Macaca mulatta*) *TTLL10* cDNA sequence was reconstructed from fragments found by NCBI Blast (http://www.ncbi.nlm.nih.gov/BLAST/) using known *TTLL10* sequences as templates. The predicted sequence was amplified from testis cDNA (BioChain Institute Inc. Hayward, CA, USA), cloned and the DNA was sequenced. PCR-related mutations were excluded by sequencing of multiple clones (complete coding sequence: Fig. S2A). For human *TTLL10*, a splice variant (Fig. S2C) of the sequence AK124125 has been amplified from testis cDNA (BioChain Institute

Inc.) and verified by DNA sequencing. *Drosophila dmTTLL3A* (CG11323) and *dmTTLL3B* (CG11201) were cloned from cDNA from adult flies.

Point mutations were introduced by a PCR-based quick-change method. The presence of the mutation was verified by DNA-sequencing.

Drosophila *genetics*

Drosophila was grown on standard medium at 25°C. The w^{1118}, *UAS-IR-TTLL3B* transgenic line was obtained from the Vienna Drosophila RNAi Center (www.vdrc.at). The transgene, localized on the X chromosome, expresses an inverted repeat from the *dmTTLL3B* gene (*CG11201*) under the control of *UAS* sequences. *UAS-IR-TTLL3B* flies were crossed with strains carrying the *da-Gal4* or the *Act5C-Gal4* driver. For amplification of the RNAi-effect, the *da-Gal4* transgene was associated with the *UAS-Dcr-2* transgene (Dietzl et al., 2007), and the resulting strain was crossed with *UAS-IR-TTLL3B* flies. Total RNA was extracted from adult flies with TRIZOL reagent (Sigma), and reverse transcription was performed using the First-Strand cDNA synthesis kit (GE Healthcare) with 5 µg of RNA and random hexamers as primers. 1/60 of this cDNA was used for PCR amplification. Primer pairs used for the detection of different gene transcripts can be provided on request. Number of PCR-cycles used for RT-PCR: RNAi, dmTTLL3B: 30, dmTTLL3A: 35, rp49: 25. Male fertility was tested in individual crosses with w^{1118} females, and the presence of progeny was scored after 2 weeks.

Isolation of axonemes from Tetrahymena cilia

CU427 *Tetrahymena* cells were grown in SPP medium (1% proteose peptone, 0.2% glucose, 0.1% yeast extract, 0.003% EDTA ferric sodium salt) at 30°C to mid log

phase (4-5x10^5 cells/ml). Cilia were collected as described (Brown et al., 1999) and stored at -80°C. For the preparation of axonemes, cilia were demembranated using 0.2% NP40 in 1x ERB buffer (50 mM Tris/HCl, pH 8.0, 10% glycerol, 5 mM $MgCl_2$, 1 mM EGTA). To remove the endogenous glycylase activity, axonemes were further treated with 1 M NaCl in 1x ERB for 30 min, followed by an incubation at 60°C for 20 min. Axonemes were spun down (12,000 g, 30 min, 4°C), and the supernatant was discarded. The pellet was then washed in 1x ERB and resuspended in 1x ERB at a final concentration of 5 mg/ml.

Tubulin polyglycylation assay

The enzymatic activity of glycylase was determined based on incorporation of [^{3}H]-glycine into MTs. The assay was performed in 50 µl of 1x ERB supplemented with 2 mM ATP and 250 pmol (5 µl) [^{3}H]-glycine (20.0 Ci/mmol, GE Healthcare). Enzymatic activity was measured using cells extracts prepared in 1x ERB containing 0.2% NP-40. 20 µg of axonemal or taxotere-stabilized MTs (prepared from adult mouse brains as described; Regnard et al., 1999) were resuspended in the reaction mixture and immediately transferred to 30°C, followed by 4 h of incubation. The samples were then subjected to SDS-PAGE (10% gels) and electrotransferred onto nitrocellulose membrane. The tubulin bands were visualized by staining with Ponceau S, cut out and placed in 5 ml of scintillation liquid (Ultima Gold, Perkin Elmer) for quantification. Alternatively, SDS-PAGE gels were stained with Coomassie Blue, incubated in Amersham Amplify^{TM} (GE healthcare), and [^{3}H]-glycine incorporation was visualized by autoradiography.

Affinity-purification of EYFP-tagged proteins

EYFP-tagged potential substrates were co-expressed with TTLL8 in HEK293 cells. After lyses of the cells in PBS, 0.2% NP40, the supernatant (100,000 g, 30 min, 4°C) was incubated with GFP-TRAP® agarose beads (ChromoTek, Martinsried, Germany) for 4 h at 4°C. Beads were washed twice in PBS, 0.2% NP40 and boiled in Laemmli sample buffer for 5 min. The samples were spun at 20,000 g for 5 min and supernatants were analyzed by SDS-PAGE and immunoblot.

Protein electrophoresis and immunoblot

One-dimensional SDS-PAGE was performed using standard protocols, or a special protocol for the separation of mammalian α- and β-tubulin (Eddé et al., 1987). Two-dimensional electrophoresis consisted of an isolelectric focusing step (IPGphor Isoelectric Focusing System; GE Healthcare) and a SDS-PAGE. For the resolution of the tubulin in Fig. 1B, 40 µg of tubulin were loaded on 18 cm pH 4.5-5.5 Immobiline strips (GE Healthcare). Cell extracts shown in Fig. 2C were prepared directly in the loading buffer (7 M urea, 2 M thiourea, 4% (w/v) CHAPS, 2% (v/v) IPG buffer (GE Healthcare), 40 mM DTT) and resolved in 8.5 cm pH 3.0-5.6 Immobiline strips (GE Healthcare).

Membranes were incubated with the following antibodies: polyG (1:6,000), polyE (1:1,000; both courtesy of M. Gorovsky), TAP952 (Bré et al., 1998; ascitic fluid, 1:2,000), 12G10 (Thazhath et al., 2002; 1:250), E7 (Chu and Klymkowsky, 1989; 1:20), 12CA5 (1:10), anti-GFP (1:5,000; Torrey Pines Biolabs), anti-NAP 4A8 (Fujii-Nakata et al., 1992; Ishimi et al., 1985; 1:20). Antibodies against TTLL8 were raised in rabbits with bacterially expressed protein, and then purified on recombinant TTLL8 and used at 1:500 dilution.

Protein bands were visualized with HRP-labeled donkey anti-rabbit or anti-mouse IgG 1:10,000 (GE healthcare) followed by detection with ECL immunoblot detection kit (GE Healthcare).

Immunofluorescence and microscopy

U2OS cells were cultured on glass coverslips under standard conditions and fixed using a protocol for preservation of cytoskeletal structures (Bell and Safiejko-Mroczka, 1995). Fixed cells were incubated with TAP952 (hybridoma supernatant 1:200), polyG (1:3,000), anti-TTLL8 (1:1,000) or anti-GST (1:1,000) antibody for 1 h, followed by 30 min with anti-mouse or anti-rabbit Alexa 555 or Alexa 488 antibody (1:1,000; Molecular Probes). DNA was visualized by DAPI staining (0.02 µg/ml). Coverslips were mounted with MOWIOL. *Drosophila* testes were fixed for 30 min with 3,7% paraformaldehyde in PBS, permeabilized in PBS containing 0.5% Triton X100, and incubated with polyG (1:9,000) for 1 h, followed by 30 min anti-rabbit Alexa 647. Actin was visualized with TRITC-conjugated phalloidin (1:10,000; Sigma). We used DMRA microscopes (Leica, Germany) and Metamorph (Universal Imaging Corp., USA) software.

For ultrastructural analysis, testes were isolated from 3-4 days old male flies and fixed in 3.5% glutaraldehyde in 100 mM phosphate buffer, pH 7.4 overnight at 4°C. The samples were rinsed in phosphate buffer and post-fixed in 1% osmic and 0.8% potassium ferrocyanide for 2 h in the dark at RT. After rinsing in phosphate buffer, samples were dehydrated in a series of ethanol solutions (30-100%) and embedded in EmBed 812 DER 736. 85 nm sections were cut on a Leica-Reichert Ultracut E microtome and counterstained with uranyl acetate and lead citrate. Images were aquired

with a Hitachi 7100 transmission electron microscope at the Centre de Ressources en Imagerie Cellulaire de Montpellier (France).

References:

Bell, P.B., Jr., and Safiejko-Mroczka, B. (1995). Improved methods for preserving macromolecular structures and visualizing them by fluorescence and scanning electron microscopy. Scanning Microsc *9*, 843-857.

Bré, M.H., Redeker, V., Quibell, M., Darmanaden-Delorme, J., Bressac, C., Cosson, J., Huitorel, P., Schmitter, J.M., Rossier, J., Johnson, T.*, et al.* (1996). Axonemal tubulin polyglycylation probed with two monoclonal antibodies: widespread evolutionary distribution, appearance during spermatozoan maturation and possible function in motility. J Cell Sci *109*, 727-738.

Bré, M.H., Redeker, V., Vinh, J., Rossier, J., and Levilliers, N. (1998). Tubulin polyglycylation: differential posttranslational modification of dynamic cytoplasmic and stable axonemal microtubules in Paramecium. Mol Biol Cell *9*, 2655-2665.

Bressac, C., Bré, M.H., Darmanaden-Delorme, J., Laurent, M., Levilliers, N., and Fleury, A. (1995). A massive new posttranslational modification occurs on axonemal tubulin at the final step of spermatogenesis in Drosophila. Eur J Cell Biol *67*, 346-355.

Brown, J.M., Marsala, C., Kosoy, R., and Gaertig, J. (1999). Kinesin-II is preferentially targeted to assembling cilia and is required for ciliogenesis and normal cytokinesis in Tetrahymena. Mol Biol Cell *10*, 3081-3096.

Chu, D.T., and Klymkowsky, M.W. (1989). The appearance of acetylated alpha-tubulin during early development and cellular differentiation in Xenopus. Dev Biol *136*, 104-117.

Dietzl, G., Chen, D., Schnorrer, F., Su, K.C., Barinova, Y., Fellner, M., Gasser, B., Kinsey, K., Oppel, S., Scheiblauer, S.*, et al.* (2007). A genome-wide transgenic RNAi library for conditional gene inactivation in Drosophila. Nature *448*, 151-156.

Dossou, S.J.Y., Bré, M.-H., and Hallworth, R. (2007). Mammalian cilia function is independent of the polymeric state of tubulin glycylation. Cell Motil Cytoskeleton *64*, 847-855.

Duan, J., and Gorovsky, M.A. (2002). Both carboxy-terminal tails of alpha- and beta-tubulin are essential, but either one will suffice. Curr Biol *12*, 313-316.

Eddé, B., de Néchaud, B., Denoulet, P., and Gros, F. (1987). Control of isotubulin expression during neuronal differentiation of mouse neuroblastoma and teratocarcinoma cell lines. Dev Biol *123*, 549-558.

Eddé, B., Rossier, J., Le Caer, J.P., Desbruyères, E., Gros, F., and Denoulet, P. (1990). Posttranslational glutamylation of alpha-tubulin. Science *247*, 83-85.

Ersfeld, K., Wehland, J., Plessmann, U., Dodemont, H., Gerke, V., and Weber, K. (1993). Characterization of the tubulin-tyrosine ligase. J Cell Biol *120*, 725-732.

Fabrizio, J.J., Hime, G., Lemmon, S.K., and Bazinet, C. (1998). Genetic dissection of sperm individualization in Drosophila melanogaster. Development *125*, 1833-1843.

Fujii-Nakata, T., Ishimi, Y., Okuda, A., and Kikuchi, A. (1992). Functional analysis of nucleosome assembly protein, NAP-1. The negatively charged COOH-terminal region is not necessary for the intrinsic assembly activity. J Biol Chem *267*, 20980-20986.

Ikegami, K., Horigome, D., Mukai, M., Livnat, I., MacGregor, G.R., and Setou, M. (2008). TTLL10 is a protein polyglycylase that can modify nucleosome assembly protein 1. FEBS Lett *582*, 1129-1134.

Ishimi, Y., Sato, W., Kojima, M., Sugasawa, K., Hanaoka, F., and Yamada, M. (1985). Rapid purification of nucleosome assembly protein (NAP-I) and production of monoclonal antibodies against it. Cell Struct Funct *10*, 373-382.

Janke, C., Rogowski, K., Wloga, D., Regnard, C., Kajava, A.V., Strub, J.-M., Temurak, N., van Dijk, J., Boucher, D., Van Dorsselaer, A.*, et al.* (2005). Tubulin polyglutamylase enzymes are members of the TTL domain protein family. Science *308*, 1758-1762.

Kann, M.L., Prigent, Y., Levilliers, N., Bré, M.H., and Fouquet, J.P. (1998). Expression of glycylated tubulin during the differentiation of spermatozoa in mammals. Cell Motil Cytoskeleton *41*, 341-352.

Lalle, M., Salzano, A.M., Crescenzi, M., and Pozio, E. (2006). The Giardia duodenalis 14-3-3 Protein Is Post-translationally Modified by Phosphorylation and Polyglycylation of the C-terminal Tail. J Biol Chem *281*, 5137-5148.

Levilliers, N., Fleury, A., and Hill, A.M. (1995). Monoclonal and polyclonal antibodies detect a new type of post-translational modification of axonemal tubulin. J Cell Sci *108*, 3013-3028.

Mans, D.A., Voest, E.E., and Giles, R.H. (2008). All along the watchtower: is the cilium a tumor suppressor organelle? Biochim Biophys Acta *1786*, 114-125.

Michaud, E.J., and Yoder, B.K. (2006). The primary cilium in cell signaling and cancer. Cancer Res *66*, 6463-6467.

Nogales, E. (2000). Structural insights into microtubule function. Annu Rev Biochem *69*, 277-302.

Redeker, V., Levilliers, N., Schmitter, J.M., Le Caer, J.P., Rossier, J., Adoutte, A., and Bré, M.H. (1994). Polyglycylation of tubulin: a posttranslational modification in axonemal microtubules. Science *266*, 1688-1691.

Redeker, V., Levilliers, N., Vinolo, E., Rossier, J., Jaillard, D., Burnette, D., Gaertig, J., and Bré, M.H. (2005). Mutations of tubulin glycylation sites reveal cross-talk between the C termini of alpha- and beta-tubulin and affect the ciliary matrix in Tetrahymena. J Biol Chem *280*, 596-606.

Regnard, C., Desbruyères, E., Denoulet, P., and Eddé, B. (1999). Tubulin polyglutamylase: isozymic variants and regulation during the cell cycle in HeLa cells. J Cell Sci *112*, 4281-4289.

Regnard, C., Desbruyères, E., Huet, J.C., Beauvallet, C., Pernollet, J.C., and Eddé, B. (2000). Polyglutamylation of nucleosome assembly proteins. J Biol Chem *275*, 15969-15976.

Schneider, A., Plessmann, U., and Weber, K. (1997). Subpellicular and flagellar microtubules of Trypanosoma brucei are extensively glutamylated. J Cell Sci *110*, 431-437.

Sjöblom, T., Jones, S., Wood, L.D., Parsons, D.W., Lin, J., Barber, T.D., Mandelker, D., Leary, R.J., Ptak, J., Silliman, N.*, et al.* (2006). The consensus coding sequences of human breast and colorectal cancers. Science *314*, 268-274.

Thazhath, R., Liu, C., and Gaertig, J. (2002). Polyglycylation domain of beta-tubulin maintains axonemal architecture and affects cytokinesis in Tetrahymena. Nat Cell Biol *4*, 256-259.

van Dijk, J., Rogowski, K., Miro, J., Lacroix, B., Eddé, B., and Janke, C. (2007). A targeted multienzyme mechanism for selective microtubule polyglutamylation. Mol Cell *26*, 437-448.

van Dijk, J., Miro, J., Strub, J.-M., Lacroix, B., Van Dorsselaer, A., Eddé, B., and Janke, C. (2008). Polyglutamylation Is a Post-translational Modification with a Broad Range of Substrates. J Biol Chem *283*, 3915-3922.

Vinh, J., Langridge, J.I., Bré, M.H., Levilliers, N., Redeker, V., Loyaux, D., and Rossier, J. (1999). Structural characterization by tandem mass spectrometry of the posttranslational polyglycylation of tubulin. Biochemistry *38*, 3133-3139.

Wloga, D., Rogowski, K., Sharma, N., Van Dijk, J., Janke, C., Eddé, B., Bré, M. H., Levilliers, N., Redeker, V., Duan, J.*, et al.* (2008). Glutamylation on alpha-tubulin is not essential but affects the assembly and functions of a subset of microtubules in Tetrahymena thermophila. Eukaryotic cell *7*, 1362-1372.

Wloga, D., Webster, D., Rogowski, K., Bré, M.-H., Levilliers, N., Jerka-Dziadosz, M., Janke, C., Dougan, S.T., and Gaertig, J. (2009). TTLL3 protein generates tubulin glycylation and regulates ciliogenesis. Dev. Cell, in press

Xia, L., Hai, B., Gao, Y., Burnette, D., Thazhath, R., Duan, J., Bré, M.H., Levilliers, N., Gorovsky, M.A., and Gaertig, J. (2000). Polyglycylation of tubulin is essential and affects cell motility and division in Tetrahymena thermophila. J Cell Biol *149*, 1097-1106.

Xie, R., Clark, K.M., and Gorovsky, M.A. (2007). Endoplasmic reticulum retention signal-dependent glycylation of the hsp70/grp170-related pgp1p in tetrahymena. Eukaryot Cell *6*, 388-397.

Acknowledgements:

This work was supported by the CNRS, the Universities Montpellier 2 and 1, the Association pour la Recherche sur le Cancer (ARC) awards CR504/7817 and 3140 (to CJ) and 4894 (to FJ), the French National Research Agency (ANR) award JC05_42022 to CJ and by the Ligue contre le Cancer fellowship JG/VP-5454, the EMBO long-term fellowship ALTF 546-2006 to KR and NSF grant MBC-033965 to JG. We thank J.-M.Donnay, G. Herrada-Aldrian, B. Lacroix, L. Linarès, J.-C. Mazur, J. Miro, D. Moustapha Abba Moussa, Y. Thomas (CRBM, Montpellier, France), V. Bäcker, J. Cau, S. DeRossi, P. Travo (RIO Imaging facility at the CRBM) and U. Rothbauer (ChromoTek GmbH, Martinsried, Germany) for technical assistance, and C. Cazevieille (CRIC, Montpellier, France) for technical assistance and helping us interpreting ultrastructural data. We are grateful to M. Bosch-Grau, A. Burgess, B. Eddé, B. Lacroix, J. Miro, A. C. Seixas (CRBM), M. Bettencourt-Dias (Instituto Gulbenkian de Ciência, Oeiras, Portugal), M. Knop, I. Mattaj (EMBL, Heidelberg, Germany) and C. Sardet (IGMM, Montpellier, France) for instructive discussions. The authors want to thank the following researchers for providing essential reagents: C. Dehay (Institute of Brain and Stem Cell Research, INSERM, Bron, France) for proving us with Rhesus sperm samples, M. Gorovsky (University of Rochester, Rochester, NY, USA) for his generous gift of the polyG and polyE antibodies, and Y. Ishimi (Mitsubishi-Kasei Institute of Life Sciences, Tokyo, Japan) for kindly providing mAb 4A8. The authors

declare no competing financial interests. The monoclonal antibody 12G10 developed by J. Frankel and M. Nelson was obtained from the Developmental Studies Hybridoma Bank developed under the auspices of the NICHD and maintained by the University of Iowa. Informed consent: human material used in this study has been obtained from persons that have agreed to participate after having been informed on the scientific background of the experiments.

Figure Legends:

Figure 1 Enzymatic characterization of murine glycylases.

(A) *In vitro* glycylation activity of TTLL3, 8 and 10 using MTs from brain that lack detectable glycylation and highly glycylated *Tetrahymena* axonemal MTs as substrates. The incorporation of [^{3}H]-glycine was separately determined for α- and β-tubulin for brain, but not for axonemal MTs due to co-migration of both tubulin subunits. **(B)** Two-dimensional analysis of α- and β-tubulin from *Tetrahymena* ciliary axonemes (12G10: anti α-tubulin; E7: anti β-tubulin). While both tubulin subunits are monoglycylated (TAP952 panel), the TTLL10-enriched fraction incorporates [^{3}H]-glycine mainly into α-tubulin *in vitro* (autoradiography panel). **(C)** Immunofluorescence analysis of U2OS cells overexpressing TTLL3-EYFP, TTLL8 or TTLL10-EYFP. TAP952 labels the MT cytoskeleton of cells expressing TTLL3 or 8, but not TTLL10. PolyG antibody detects a diffuse staining after TTLL10 overexpression. Non-transfected cells, visualized by DAPI-staining of the nuclei, are neither labeled with TAP952 nor with polyG (arrowheads). *TTLL8 was expressed as an untagged protein and detected with anti-TTLL8 antibody. Scale bar is 20 μm.

Figure 2 The cooperative mechanism of murine polyglycylases.

(A) Immunofluorescence of U2OS cells co-expressing TTLL10-ECFP together with TTLL3-EYFP or TTLL8-EYFP. Note that polyG antibody labels the cytoskeleton. Scale bar is 20 μm. **(B)** Immunoblot analysis of extracts from U2OS cells expressing TTLL3-EYFP, TTLL8 and TTLL10-6HA alone as well as TTLL3-EYFP or TTLL8 in combination with TTLL10-6HA. TAP952 recognizes protein bands exclusively in cell extracts after expression of TTLL3 or 8. Different proteins are detected with polyG antibody after overexpression of TTLL10 alone or in combination with TTLL3 or 8. **(C)** Two-dimensional electrophoresis and immunoblot of extracts from control U2OS cells (-) or cells expressing TTLL10-6HA (+). The positions of α- and β-tubulin as well as NAPs are determined with specific antibodies. (# polyglycylated NAPs; * non-specific polyG signal)

Figure 3 Evolutionary loss of polyglycylation in humans.

(A) Immunoblot analysis of mouse, rhesus and human sperm proteins. The polyG antibody detects specific protein bands in mouse and rhesus, but not in human sperm. In contrast, TAP952 detects tubulin bands at a low level in mouse and rhesus, but strongly in human. The polyE antibody labels tubulin of all three species equally strong. **(B)** Immunoblot analysis of extracts from U2OS cells expressing mouse, rhesus or human TTLL10. **(C)** *In vitro* enzymatic assay of mouse, rhesus and human TTLL10 expressed in HEK293 cells with axonemal MTs as a substrate. **(D)** Immunoblot of U2OS cells expressing wild type rhesus and human TTLL10, as well as human TTLL10 containing sequence reversions to amino acids present in rhesus and mouse TTLL10 (see Fig. S3): S 448 N (rev3; reversion of mut3; see Fig. S4C), K 467 T (rev5; reversion of mut5; see Fig. S4C), or both of them (rev3+5). Wild type rhesus TTLL10 and human TTLL10

carrying both rev3 and rev5 generated a strong polyG signal on NAPs, indicative of polyglycylase activity. **(E)** Schematic representation of the human TTLL10 protein indicating the localization of the two amino acid reversions that allowed for re-activation of polyglycylase activity. The localization of the conserved core TTL domain (yellow) and the essential ATP-binding residue E511 are indicated (red; Fig. S3; van Dijk et al., 2007).

Figure 4 Loss of enzymatic activity of TTLL3 in colon cancer.

(A) Sequence alignment of different TTLL proteins from different organisms maps the position of two cancer-related mutations in TTLL3 (G647S: green, M669I: pink; Sjöblom et al., 2006) to two highly conserved positions in the vicinity of the major ATP binding site (E662, yellow). Amino acids in red letters: homology, in blue: similarity. **(B)** TAP952 labeling of U2OS cells expressing wild type TTLL3-EYFP and the mutated proteins including the E622G ATPase dead version. Scale bar is 20 µm. **(C)** Immunoblot of extracts from U2OS cells expressing wild type and mutated TTLL3s. **(D)** *In vitro* glycylation assay of extracts from HEK293 cells expressing either the wild type or mutated forms of TTLL3 using brain MTs as substrate.

Figure 5 The enzymatic mechanism of polyglycylation in *Drosophila*.

(A) Immunofluorescence analysis of U2OS cells expressing *Drosophila melanogaster* (dm) TTLL3A-EYFP and TTLL3B-EYFP proteins. TAP952 labels cytoskeletal structures in cells expressing either of these proteins; however, some cells with a dominant nuclear localization of dmTTLL3B (#) show only diffuse nuclear labeling with this antibody. PolyG decorates the cytoskeleton in cells expressing dmTTLL3A, but only the nucleus in the cells that express dmTTLL3B. Non-transfected

cells are visualized by DAPI-staining of the nuclei. Scale bar is 20 µm. **(B)** Immunoblot analysis of extracts from U2OS cells expressing dmTTLL3A and dmTTLL3B. Both enzymes generate specific labeling of protein bands with the TAP952 and polyG antibodies. (* non-specific polyG signal)

Figure 6 Effects of dmTTLL3B depletion in *Drosophila*.

(A) Comparison of the survival of female and male flies carrying *UAS-IR-dmTTLL3B* transgene in the presence or absence of the driver. The percentage of viable adult flies as compared to the number of embryos is shown. **(B)** RT-PCR analysis of *dmTTLL3B*-RNAi, *dmTTLL3B*, *dmTTLL3A* and *rp49* expression in control (*da-Gal4/+*) and $dmTTLL3B^{da\text{-}RNAi}$ flies. **(C)** Immunoblots of whole-fly extracts, probed for polyglycylation (polyG), polyglutamylation (GT335) and α-tubulin (12G10). In control (*da-Gal4/+*) flies, multiple proteins are labeled with polyG antibody in male and female flies. This labeling is strongly reduced in $dmTTLL3B^{da\text{-}RNAi}$ flies. In contrast, polyglutamylation is only detected in male individuals, and increases upon depletion of polyglycylation. **(D)** Sterility of male flies carrying *UAS-IR-dmTTLL3B* transgene in the presence or absence of the driver. **(E)** Immunofluorescence of testes from control (*da-Gal4/+*) and $dmTTLL3B^{da\text{-}RNAi}$ flies. Actin is stained with TRITC-conjugated phalloidin (red), and polyglycylated proteins are revealed with polyG antibody (green). Nuclei are stained with DAPI (blue). In $dmTTLL3B^{da\text{-}RNAi}$ flies, polyglycylation levels are decreased and actin cones are scattered. The tip of the testes (arrowhead) is enlarged. Insets show the distribution of actin cones (zoom 2.5x). Scale bar is 100 µm. **(F** and **G)** Transmission electron micrographs of sections of cysts from control (*da-Gal4/+*) and $dmTTLL3B^{da\text{-}RNAi}$ flies. Red arrowheads show axonemes, blue mitochondria. Scale bar is 500 nm. **(F)** Immature cysts of $dmTTLL3B^{da\text{-}RNAi}$ flies show no phenotypic abnormalities

as compared to control. **(G)** Phenotype of mature cysts in control and *dmTTLL3B*$^{da\text{-}RNAi}$ flies. Abnormalities found in *dmTTLL3B*$^{da\text{-}RNAi}$ flies include reduced number of mitochondria, disorganized axoneme structures (singlet microtubules; inset with 2.5x zoom) and complete absence of axonemes.

Figure 7 New substrates of glycylation.

EYFP-tagged mouse or *Drosophila* proteins were co-expressed with active (A) or inactive ("dead"; D) mouse TTLL8 in HEK293 cells. After EYFP affinity purification proteins were detected with anti-GFP antibody, and the level of glycylation was determined with TAP952. The total extract was probed for TTLL8 expression with anti-TTLL8 antibody.

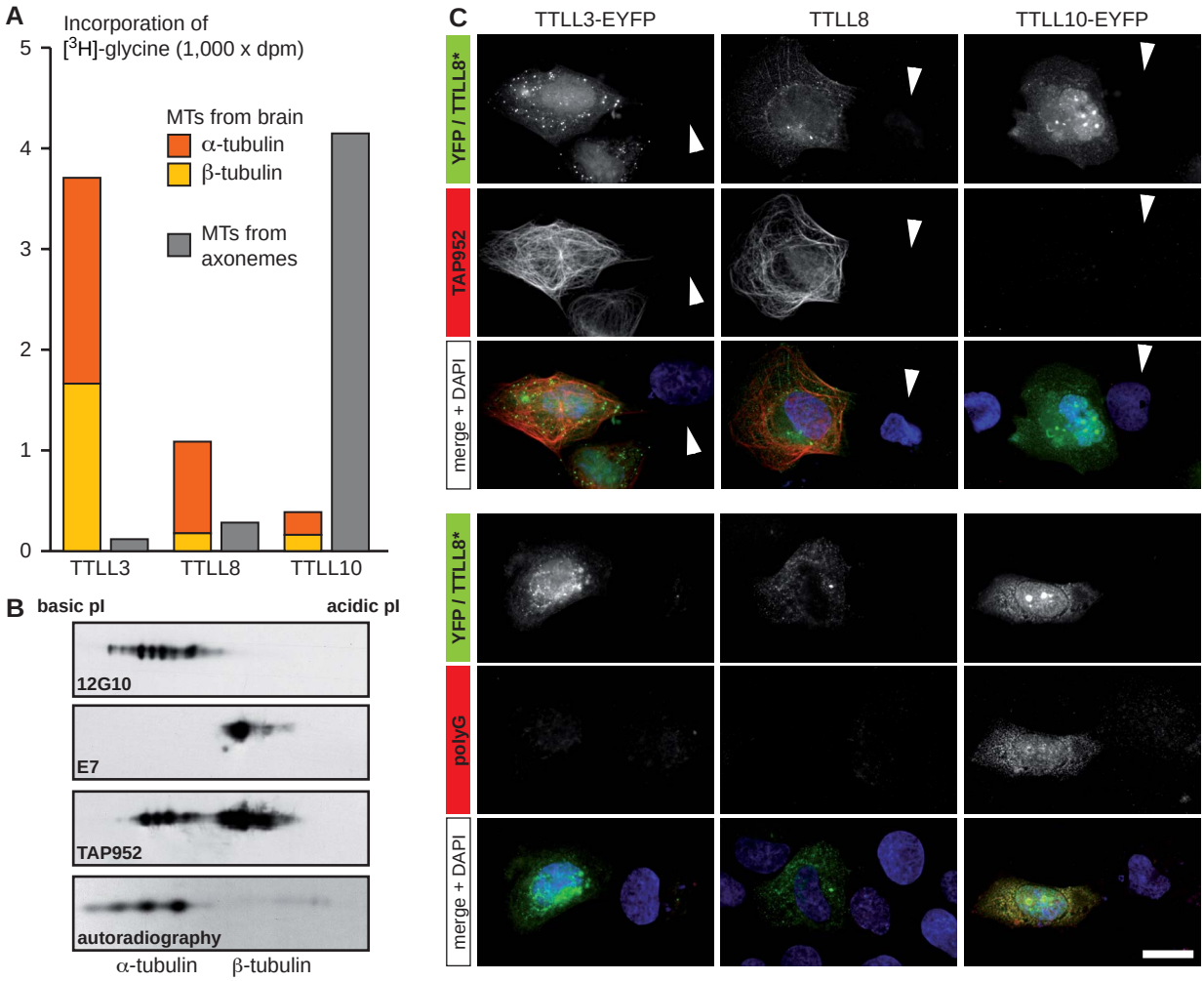
A
Incorporation of
[3H]-glycine (1,000 x dpm)
5
4
3
2
1
0
MTs from brain
α-tubulin
β-tubulin
MTs from
axonemes
TTLL3
TTLL8
TTLL10
B
basic pI
acidic pI
12G10
E7
TAP952
autoradiography
α-tubulin
β-tubulin
C
TTLL3-EYFP
TTLL8
TTLL10-EYFP
YFP / TTLL8*
TAP952
merge + DAPI
YFP / TTLL8*
polyG
merge + DAPI

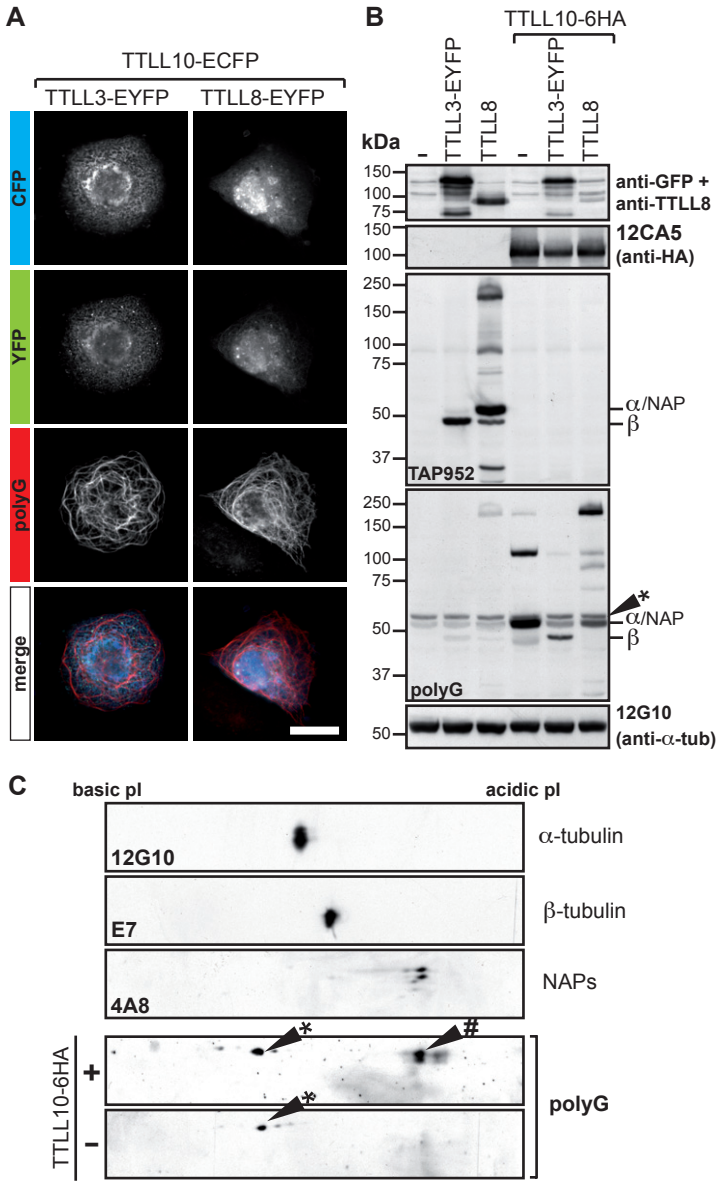
A
TTLL10-ECFP
TTLL3-EYFP
TTLL8-EYFP
CFP
YFP
polyG
merge
B
TTLL10-6HA
TTLL3-EYFP
TTLL8
kDa
anti-GFP +
anti-TTLL8
12CA5
(anti-HA)
α/NAP
β
TAP952
polyG
12G10
(anti-α-tub)
C
basic pI
acidic pI
12G10
α-tubulin
E7
β-tubulin
4A8
NAPs
TTLL10-6HA
polyG

Rogowski et al., Figure 3

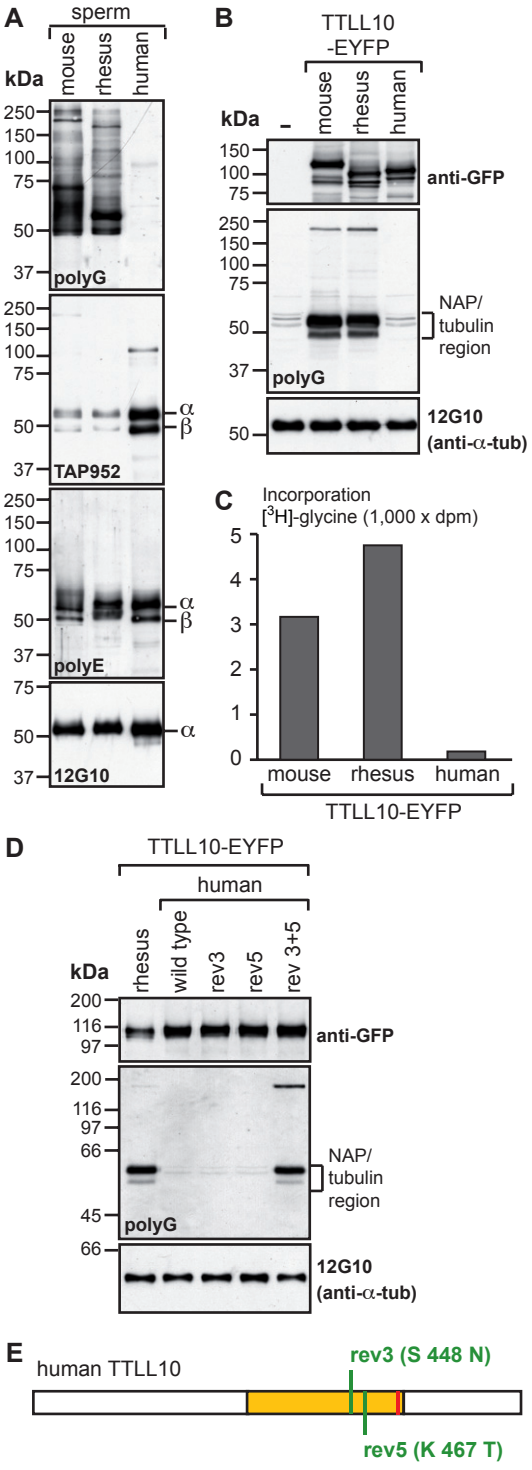

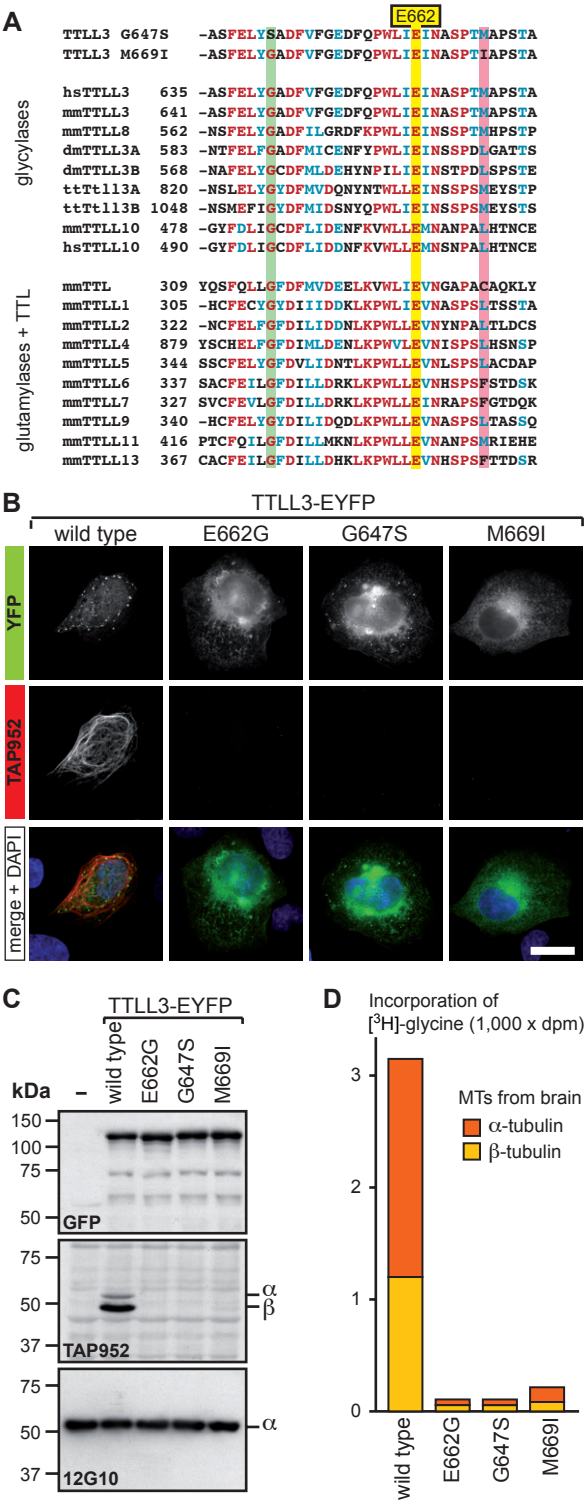
A
E662
TTLL3 G647S -ASFELYSADFVFGEDFQPWLIEINASPTMAPSTA
TTLL3 M669I -ASFELYGADFVFGEDFQPWLIEINASPTIAPSTA
glycylases
hsTTLL3 635 -ASFELYGADFVFGEDFQPWLIEINASPTMAPSTA
mmTTLL3 641 -ASFELYGADFVFGEDFQPWLIEINASPTMAPSTA
mmTTLL8 562 -NSFELYGADFILGRDFKPWLIEINSSPTMHPSTP
dmTTLL3A 583 -NTFELFGADFMICENFYPWLIEINSSPDLGATTS
dmTTLL3B 568 -NAFELYGCDFMLDEHYNPILIEINSTPDLSPSTE
ttTtll3A 820 -NSLELYGYDFMVDQNYNTWLLEINSSPSMEYSTP
ttTtll3B 1048 -NSMEFIGYDFMIDSNYQPWLIEINSSPSMEYSTS
mmTTLL10 478 -GYFDLIGCDFLIDENFKVWLLEMNANPALHTNCE
hsTTLL10 490 -GYFDLIGCDFLIDDNFKVWLLEMNSNPALHTNCE
glutamylases + TTL
mmTTL 309 YQSFQLLGFDFMVDEELKVWLIEVNGAPACAQKLY
mmTTLL1 305 -HCFECYGYDIIIDDKLKPWLIEVNASPSLTSSTA
mmTTLL2 322 -NCFELFGFDILIDDNLKPWLLEVNYNPALTLDCS
mmTTLL4 879 YSCHELFGFDIMLDENLKPWVLEVNISPSLHSNSP
mmTTLL5 344 SSCFELYGFDVLIDNTLKPWLLEVNLSPSLACDAP
mmTTLL6 337 SACFEILGFDILLDRKLKPWLLEVNHSPSFSTDSK
mmTTLL7 327 SVCFEVLGFDILLDRKLKPWLLEINRAPSFGTDQK
mmTTLL9 340 -HCFELYGYDILIDQDLKPWLLEVNASPSLTASSQ
mmTTLL11 416 PTCFQILGFDILLMKNLKPWLLEVNANPSMRIEHE
mmTTLL13 367 CACFEILGFDILLDHKLKPWLLEVNHSPSFTTDSR
B
TTLL3-EYFP
wild type
E662G
G647S
M669I
YFP
TAP952
merge + DAPI
C
TTLL3-EYFP
wild type
E662G
G647S
M669I
kDa
–
150
100
75
50
GFP
75
50
37
TAP952
α
β
75
50
37
12G10
α
D
Incorporation of
[3H]-glycine (1,000 x dpm)
3
2
1
0
MTs from brain
α-tubulin
β-tubulin
wild type
E662G
G647S
M669I

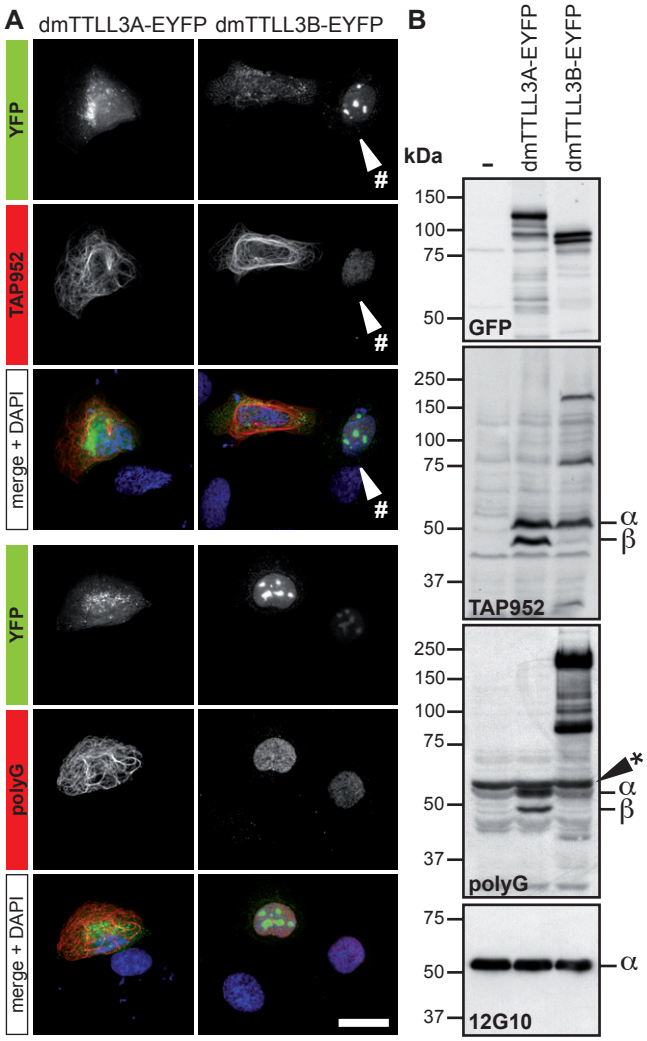
A
dmTTLL3A-EYFP
dmTTLL3B-EYFP
YFP
TAP952
merge + DAPI
YFP
polyG
merge + DAPI
#
B
kDa
–
dmTTLL3A-EYFP
dmTTLL3B-EYFP
150
100
75
50
GFP
250
150
100
75
50
37
TAP952
α
β
250
150
100
75
50
37
polyG
*
α
β
75
50
37
12G10
α

Rogowski et al., Figure 6

Rogowski et al., Figure 7

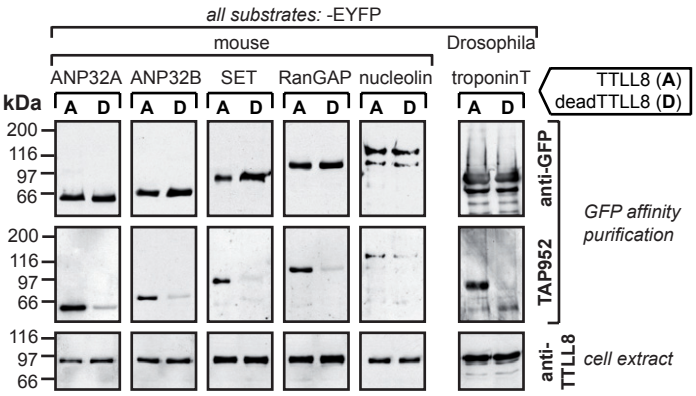

Supporting online material for:

Evolutionary divergence of enzymatic mechanisms for post-translational polyglycylation

Krzysztof Rogowski, François Juge, Juliette van Dijk, Dorota Wloga, Jean-Marc Strub, Nicolette Levilliers, Daniel Thomas, Marie-Hélène Bré, Alain Van Dorsselaer, Jacek Gaertig and Carsten Janke

This file contains:

Supplementary Figures S1, S2, S3, S4, S5, S6, Table S1, supplementary text, supplementary materials and methods, supplementary references

Table S2 is added as an extra file (Rogowski_suppl_tableS2.xls)

Supplementary figures:

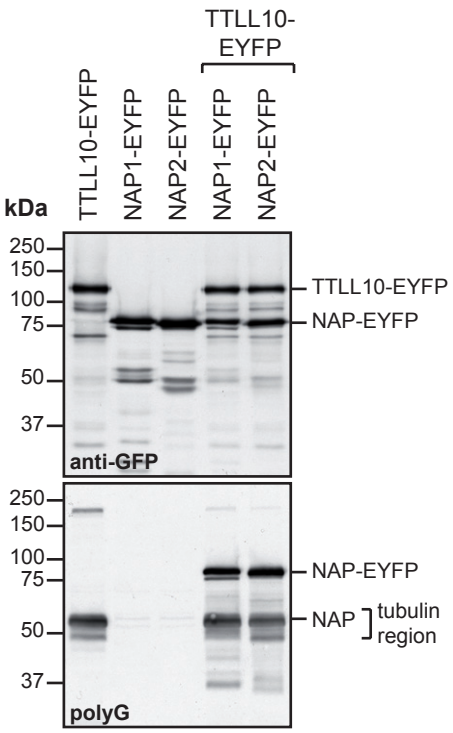

Figure S1: Exogenously expressed NAPs are polyglycylated by TTLL10

NAP1-EYFP and NAP2-EYFP were expressed alone or in combination with murine TTLL10-EYFP in U2OS cells. Upon overexpression of TTLL10-EYFP alone, the polyG antibody labels a strong protein band in the 50 kDa region, which corresponds to endogenous NAPs (Fig. 2B, C). When NAP1-EYFP or NAP2-EYFP were co-expressed with TTLL10-EYFP, polyG recognizes additional protein bands at ~75 kDa, which are identified as NAP1 and NAP2 EYFP fusion proteins using anti-GFP labeling. Thus, NAP1 and NAP2 are polyglycylated by TTLL10 (Fig. 2B, C).

A Macaca mulatta *TTLL10* mRNA ORF:

```
ATGGCCCACAGCTGCACCCGGTTCGTCCATCGCCGGGGACCGCCCACTCGGACCCAAGCCGGCTCCAAGAGGGGCAAGAGACCAAAGATCCAGCGGCGGC
CTCGGGCTCGAGTCCCAGGCCCAGCCCATGAGAGGCCAATGGGGAGCAGCCAGGAGGAGGGACTCCCGTGTCAGCCAAGCCAGCCAGACCACGACACAGA
CTCGGATGACACTGATGCCACTGGGCCCCCAGCTGCCCTCCTGGAGGGGCTCCTGCTGGGGGACGGGAAGCCATCGCCCCACAGCACGAGGCCGGGACCT
TTCTTCTACATCGGAGGCAACAACGGGGCTGCGATCATCAGCTCCTACTGCAAAAGCAAGGGCTGGCGGCGCATCCAGGACAGCCGCCGGGAGGACTATG
TGCTGAAGTGGTGTGAGGTGAAGAGCCGAGACAGCTACGGCAGCTTCCGGGAAGGAGAGCAGCTGCTGTACCAGCTTCCCAACAACAAGCTCCTCACCAC
CAAGATCGGGCTGCTCAGCACCCTTCGGGGGCGGGCATGGGCCATGAGCAAGGCCAGCAAGGCGCCGGGGGGGACCCAGGCCAGGCTGGGAAAGGACGCA
ACAGCACCCACCCTGGAGGACCTCCCGTGGACAAGCCCAGGACACCTCAGGCCACAGAGGGTCCTGAGAATGGAGGAGTTTTTCCCAGAGACCTACCGCC
TGGACCTCAAGCACGAGAGAGAGGCTTTTTTCACCCTGTTTGACGAAACCCAGATATGGATCTGCAAGCCCACGGCCTCCAACCAGGGCAAAGGCATCTT
CCTGCTCCGGAAGCAGGAGGAAGTTGCCGCCCTGCAGGCCAAGACCCGGAGCGCGGAGGACGACCCCATCCACCATAAGTCGCCGTTCCGGGGGCCTCAG
GCGCGGGTGGTGCAGAGGTATATCCAGAACCCCCTGCTGCTGGATGGGAGGAAGTTTGACGTGCGCTCCTACCTGCTCATCGCCTGCACCACACCCTACA
TGATCTTCTTCAGCCACGGCTATGCCCGCCTCACCCTCAGCCTCTATGACCCCCATTCCAGCGACCTCAGCGGCCACCTGACCAACCAGTTCATGCAGAA
GAAGAGCCCGCTGTACGTGCTGCTGAAGGAGGACACGGTGTGGAGCATGGAGCGCCTCAACCGATACATCAACACCACGTTCTGGAAAGCCCGGGGCCTC
CCCAAGGACTGGGTCTTCACCACCCTCACGAAGCGGATGCAGCAGATCATGGCCCACTGCTTTCTGGCCGCCAAGTCCAAGCTGGAGTGCAAGCTGGGTT
ACTTTGACCTCATCGGCTGTGACTTCCTGATTGATGACAACTTCAAGGTATGGCTGCTGGAGATGAATTCCAACCCAGCCCTGCACACCAACTGCGAGGT
CCTGAAGGAGGTCATCCCAGGTGTGGTCATCGAGACCCTGGACCTGGCACTGGAGACCTTCCAGAAGAGCCTGCGCGGCCAGAAGATGCTGCCTCTGCTG
TCCCAGCGTCGCTTCGTGCTCCTGCACAACGGAGAGGCCGACGTGTGGCCGCGCCTGGGGGGCTCCTGCAGCCTCCACCGACGGCTGCCTCCGCCCACCC
GCCAGGCCAAGTCCTCCGGGCCACCCACGCCGCGTGCCCCAGACCAGCCGGGCACCCGCAGGCATGTGCCACCTCCCTTGGCACCGCAGCGTCCCCAGTT
GCCCGGCCCCAGTCCTGACCCAGATAGCGCCCACGATGGGCAGCCCCAGGCCCCGGGCAAGGAGCAGTCGGGCACAGGCGACAGGCACCCGGAGCAAGAG
CCTTCCCCGGGGACAGCCAAGGAGGAACGCAAGGAGCCCGAGAACGCGAGGCCCTGGGGCGGCCACCCACGCCCCACACCCCACGCCCCAGCCACACTGC
CCGCCTTCAGGGACCTATAA
```

B *Macaca mulatta* TTLL10 protein sequence:

```
MAHSCTRFVHRRGPPTRTQAGSKRGKRPKIQRRPRARVPGPAHERPMGSSQEEGLPCQPSQPDHDTDSDDTDATGPPAALLEGLLLGDG
KPSPHSTRPGPFFYIGGNNGAAIISSYCKSKGWRRIQDSRREDYVLKWCEVKSRDSYGSFREGEQLLYQLPNNKLLTTKIGLLSTLRGR
AWAMSKASKAPGGTQARLGKDATAPTLEDLPWTSPGHLRPQRVLRMEEFFPETYRLDLKHEREAFFTLFDETQIWICKPTASNQGKGIF
LLRKQEEVAALQAKTRSAEDDPIHHKSPFRGPQARVVQRYIQNPLLLDGRKFDVRSYLLIACTTPYMIFFSHGYARLTLSLYDPHSSDL
SGHLTNQFMQKKSPLYVLLKEDTVWSMERLNRYINTTFWKARGLPKDWVFTTLTKRMQQIMAHCFLAAKSKLECKLGYFDLIGCDFLID
DNFKVWLLEMNSNPALHTNCEVLKEVIPGVVIETLDLALETFQKSLRGQKMLPLLSQRRFVLLHNGEADVWPRLGGSCSLHRRLPPPTR
QAKSSGPPTPRAPDQPGTRRHVPPPLAPQRPQLPGPSPDPDSAHDGQPQAPGKEQSGTGDRHPEQEPSPGTAKEERKEPENARPWGGHP
RPTPHAPATLPAFRDL
```

C *Homo sapiens* TTLL10 protein sequence:

```
MDHSCTRFIHRRGPPTRTRAGFKRGKRPRIQQRPRARVSG**tipasrlhpapasqpgpcpapghcpvg**PAHERPMGSSQEEGLRCQPSQP
DHDADGHCGPDLEGAERASATPGPPGLLNSHRPADSDDTNAAGPSAALLEGLLLGGGKPSPHSTRPGPFFYIGGSNGATIISSYCKSKG
WQRIHDSRRDDYTLKWCEVKSRDSYGSFREGEQLLYQLPNNKLLTTKIGLLSTLRGRARAMSKASKVPGGVQARLEKDAAAPALEDLPW
TSPGYLRPQRVLRMEEFFPETYRLDLKHEREAFFTLFDETQIWICKPTASNQGKGIFLLRNQEEVAALQAKTRSMEDDPIHHKTPFRGP
QARVVQRYIQNPLLVDGRKFDVRSYLLIACTTPYMIFFGHGYARLTLSLYDPHSSDLGGHLTNQFMQKKSPLYMLLKEHTVWSMEHLNR
YISDTFWKARGLAKDWVFTTLKKRMQQIMAHCFLAAKPKLDCKLGYFDLIGCDFLIDDNFKVWLLEMNSNPALHTNCEVLKEVIPGVVI
ETLDLVLETFRKSLRGQKMLPLLSQRRFVLLHNGEADPRPHLGDSCSLRRWPPLPTRQAKSSGPPMPHAPDQPGARRPAPPPLVPQRPR
PPGPDLDSAHDGEPQAPGTEQSGTGNRHPAQEPSPGTAKEEREEPENARP
```

Figure S2: Sequences of *Macaca mulatta* and *Homo sapiens* TTLL10.

(A) Full coding sequence of *Macaca mulatta TTLL10* according to our cloning and sequencing. PCR-related mutations have been eliminated. **(B)** Protein sequence of *Macaca mulatta* TTLL10. **(C)** Protein sequence of human TTLL10 (translation of AK124125). An alternatively spliced exon (corresponding amino acids 41-67, lower case letters) is absent in the TTLL10 we use in the present study. For simplification, the amino acid numbering according to the longest isoform of human TTLL10 is used throughout this study.

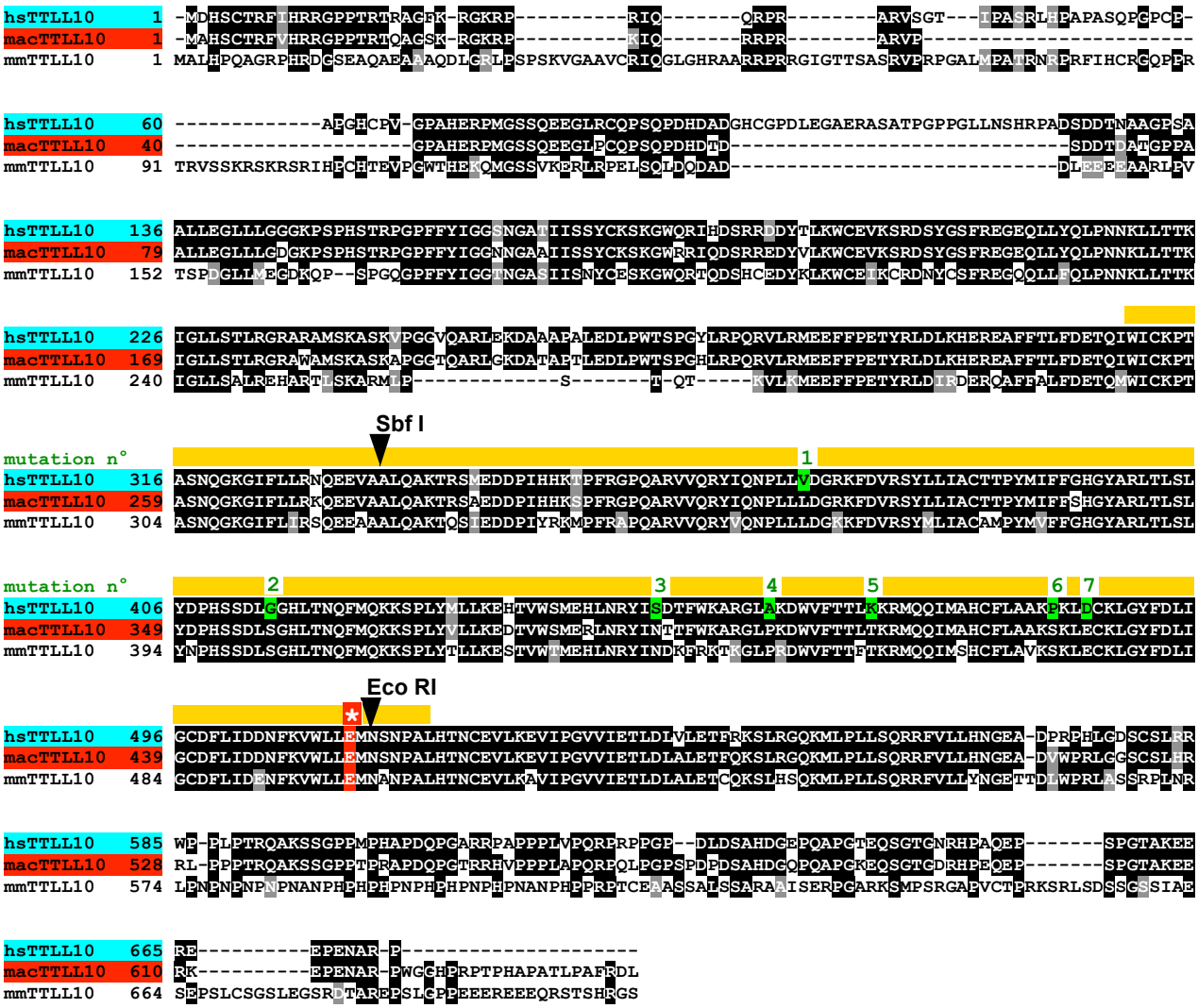

Figure S3: Sequence alignment and features of TTLL10 proteins.

The protein sequences of human (hs; longest transcript; Fig. S2C), rhesus (*Macaca mulatta*; mac) and mouse (mm) TTLL10 have been aligned with Clustal X. Amino acid homologies (black) and similarities (gray) are indicated. The central region of the proteins, corresponding to the core TTL-domain (orange box; van Dijk et al., 2007), is highly homologous, whereas the flanking N- and C-terminal regions are more divergent, notably between mouse and the two primates. For the generation of chimeras (Fig. S4A) the central domains of rhesus and human TTLL10 were exchanged using the Sbf I and Eco RI restriction sites. Within this region, only 7 specific amino acid alterations between rhesus and human TTLL10 that could be responsible for the loss of activity of the human enzyme are present (green). 4 additional alterations between the sequence of rhesus and human TTLL10 correspond to non-conserved amino acids as they were also different in the active mouse TTLL10. Thus, they were not investigated. The essential ATP-interacting residue E511 (hsTTLL10; *) is indicated in red.

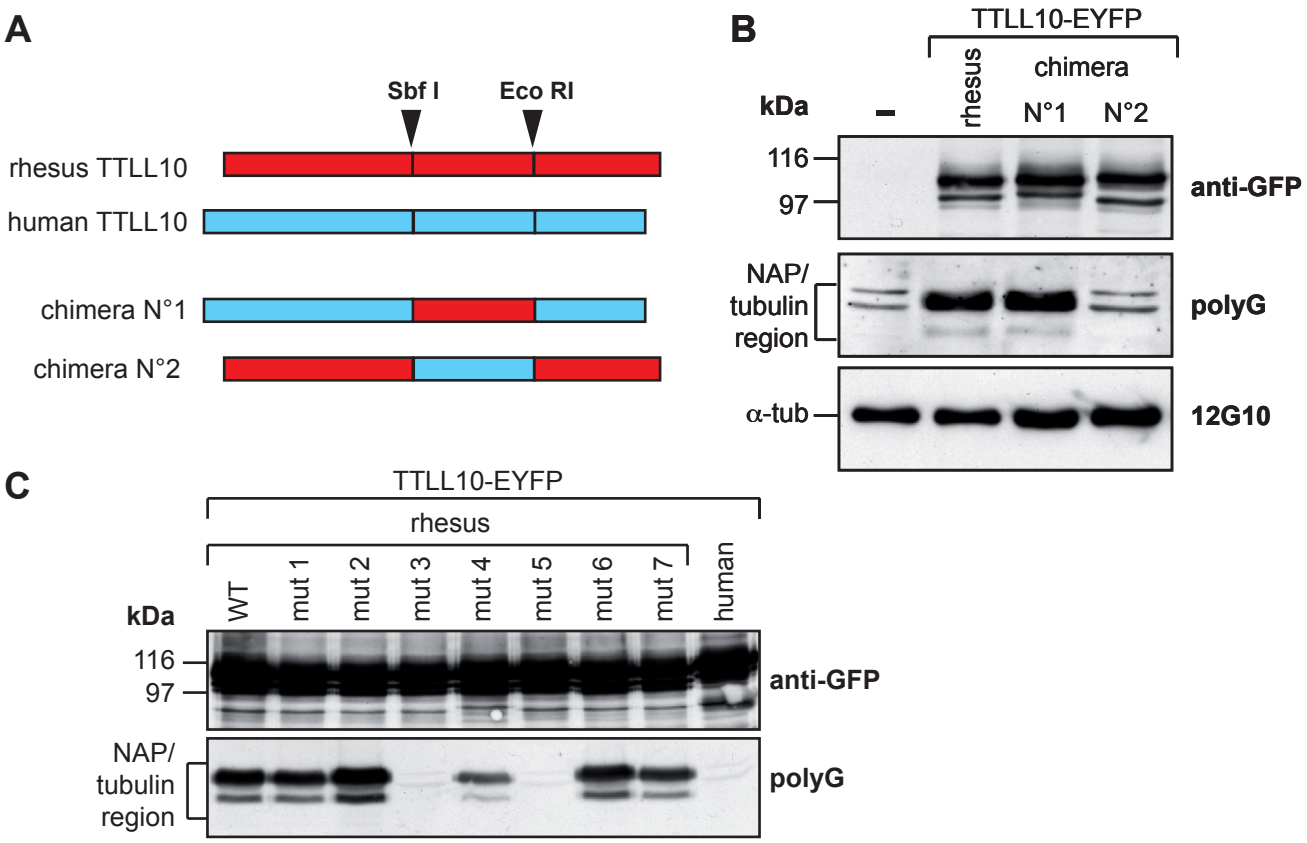

Figure S4: Mapping of the mutations that lead to the loss of enzymatic activity of human TTLL10.

(A) Schematic representation of chimeras generated by domain exchange between rhesus (red) and human (blue) *TTLL10*. The sequence positions of the exchange point are shown in Fig. S3. **(B)** To test the enzymatic activity of the respective constructs, rhesus and the chimeric TTLL10 proteins were expressed in U2OS cells. Only rhesus TTLL10 and chimera N°1 increased the polyG signal on NAPs, indicative of enzymatic activity of the proteins. This revealed that the loss of activity of human TTLL10 is related to amino acid changes in the central domain (amino acid 334-513; see Fig. S3) that corresponds approximately to the core TTL domain.

(C) To map which of the single amino acid changes lead to a loss of TTLL10 activity, the 7 conserved mutations found in human *TTLL10* (mut1-7; see Fig. S3) were separately introduced into rhesus *TTLL10*. Note that only two mutations, mut3 and 5 led to a complete loss of activity of rhesus TTLL10, as indicated by the absence of a polyG signal on immunoblot (WT: wild type).

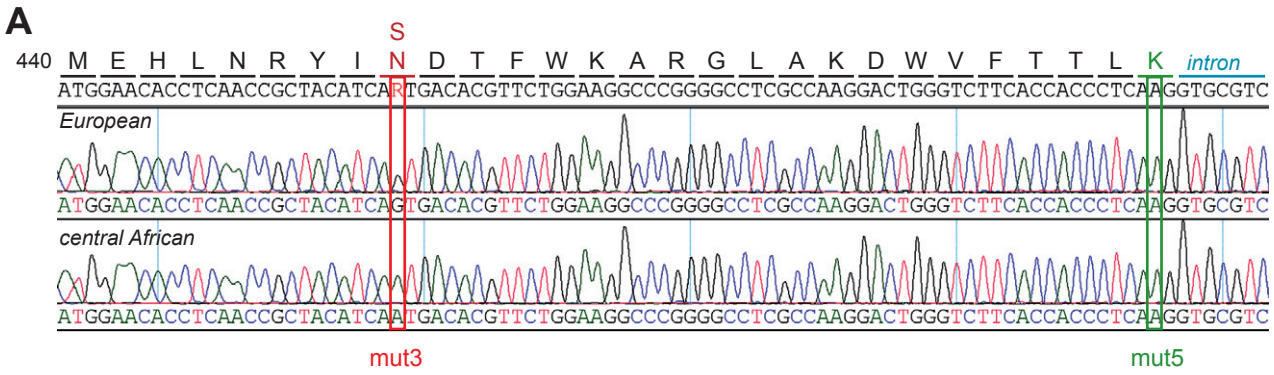

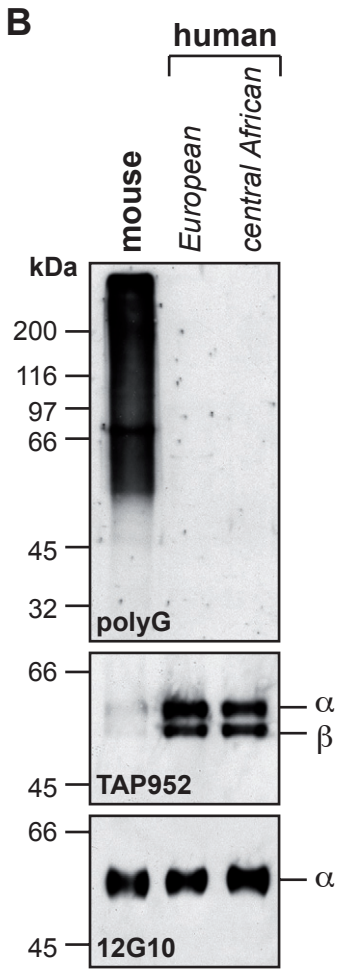

Figure S5: The polymorphism of the human *TTLL10* gene has no impact on the enzymatic activity of TTLL10 protein

(A) Alignment of DNA sequences of human genomic DNA from two individuals with European and central African origins. The mutation A1343G (mut3; nucleic acid count of the *TTLL10* open reading frame), which introduces a N448S amino acid change into TTLL10 in individuals of European origin is absent in the *TTLL10* gene of an individual of central African origin. In contrast, the mutation C1400A (T467K) is present in both individuals. Statistic data on the distribution of this polymorphism in the human population can be found at: http://www.ncbi.nlm.nih.gov/SNP/snp_ref.cgi?rs=1320571

(B) Immunoblot of mouse and human (European and central African) sperm protein with polyG (polyglycylation), TAP952 (monoglycylation) and 12G10 (α-tubulin). Despite the polymorphism in mut3 (A), both human individuals have no polyglycylation (polyG), instead strong monoglycylation was detected on α- and β-tubulin (TAP952).

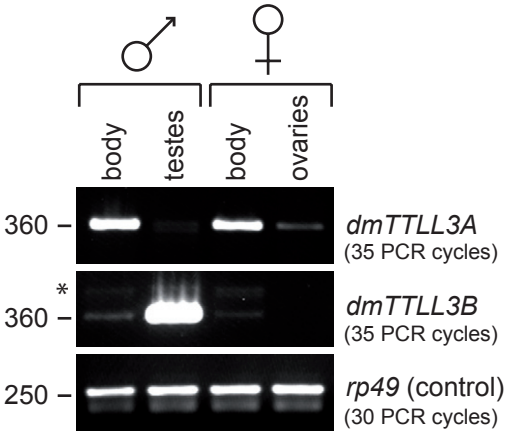

Figure S6: Tissue-specific expression of the *Drosophila melanogaster TTLL3A* and *TTLL3B* genes

RT-PCR analysis of *dmTTLL3A* and *dmTTLL3B* in wild type flies. In male flies, testes were dissected from remaining body tissue and analyzed separately. Similarly, the ovaries and the body were analyzed from female flies. *dmTTLL3A* is expressed at moderate levels in the bodies of both, male and female flies, but very low expression levels are detected in testes and ovaries. In contrast, *dmTTLL3B* is highly expressed in testes, but at very low levels in other tissues (body). No *dmTTLL3B* expression was detected in ovaries.

The results are in agreement with published microarray expression data:

dmTTLL3A: http://flyatlas.org/atlas.cgi?name=FBgn0031854

dmTTLL3B: http://flyatlas.org/atlas.cgi?name=FBgn0031853.

(* contaminating PCR product from genomic DNA)

Supplementary tables:

Table S1: Summary of the proteins identified in the major polyG-reactive protein spots after two-dimensional gel electrophoresis (proteins chosen for further analysis are in bold letters)

spot N°	*protein name*	*accession N°*	*gene*	*molecular weight (Da)*	*N° of pep-tides*	*RMS*	*score*	*sequence coverage*
1	aldehyde dehydrogenase	gi|20129399	CG3752	56,983	25	5	1797	57%
	amino peptidase	gi|21355725	CG6372	61,474	11	3	729	24%
	RPT1	**gi|17137738**	**CG1341**	**48,525**	**7**	**4**	**398**	**18%**
	ERp60	gi|45445579	CG8983	55,235	10	2	482	28%
	TCP1η	gi|23170738	CG8351	54,835	3	4	176	7%
	NADH-ubiquinone reductase	gi|17933656	CG6343	46,868	2	3	156	9%
	aldehyde dehydrogenase	gi|24650465	CG31075	52,573	4	3	188	9%
	enolase	gi|7946	CG17654	46,534	3	2	145	11%
	EF-1α	gi|7915	CG8280	50,250	2	4	99	4%
2	HSP60C	gi|21064097	CG7235	61,570	28	6	2024	59%
	TCP1β	**gi|18858175**	**CG7033**	**58,047**	**20**	**3**	**1515**	**52%**
	α1 tubulin	gi|17865841	CG9476	49,890	10	3	687	26%
	FK506-binding protein	gi|24583150	CG4535	48,765	7	4	306	17%
	homolog of lipase	gi|24642748	CG18258	51,135	2	8	141	4%
	homolog of leucine amino-peptidase 3	gi|24661038	CG32351	61,333	2	4	144	5%
	hu-li tai shao protein	gi|157747	CG9325	127,873	2	6	114	3%
	homolog of xylulokinase	gi|21356607	CG3534	61,115	3	2	113	6%
3	**paramyosin**	**gi|10959**	**CG5939**	**102,322**	**46**	**4**	**3291**	**61%**
	HSP60C	gi|21064097	CG7235	61,520	3	3	263	10%
	HSC70Cb	**gi|21357475**	**CG6603**	**88,484**	**4**	**2**	**191**	**6%**
4	**HSP60B**	**gi|15010456**	**CG2830**	**68,620**	**35**	**3**	**2680**	**64%**
5	HSP60A	gi|33636453	CG12101	60,778	43	6	1643	76%
	esterase 6	gi|1832142	CG6917	61,109	10	4	646	23%
	CG4546p	gi|24647265	CG4546	52,111	4	6	275	10%
6	ATP synthase β	gi|24638766	CG11154	54,091	26	6	877	76%
	β2 tubulin	gi|158743	CG9359	49,826	6	6	361	52%
	β3 tubulin	gi|158749	CG3401	50,882	4	5	234	36%
	β4 tubulin	gi|21428640	CG4869	51,220	2	7	164	10%
	loopin-1	gi|20130057	CG4750	56,686	3	3	259	7%
	upheld (troponinT)	**gi|38570263**	**CG7107**	**47,431**	**4**	**2**	**259**	**12%**

Table S2: Complete mass spectrometry data of selected proteins; see attached file Rogowski_suppl_tableS2.xls

Supplementary text:

To identify new substrates of polyglycylation form *Drosophila* testes, we resolved testes protein extracts using two-dimensional gel electrophoresis. The gel was stained with Coomassie brilliant blue, and in parallel immunoblots with polyG were performed from similar gel. Comparing the immunoblots to the stained gel, we identified 6 prominent spots that were labeled with polyG, and submitted these spots to mass spectrometry for protein identification. From the proteins that were identified in each spot (Table S1), we selected in most cases proteins with a high score for further analysis. Different paralogs of HSP60 were identified in several spots. We focused on HSP60B, since it has been the only protein detected in spot n°4. From spot n°1, we decided to select only RPT1, based on the consideration that the function of this protein as a subunit of the 26S proteasome could be important for sperm maturation (Zhong and Belote, 2007). From spot n°2 we chose TCP1β. From spot n°3 we chose all proteins except for the HSP60 paralog, whereas we decided not to analyze any protein from spot n°5. Spot n°6 was rich in β-tubulins, suggesting that the detected polyG signal was generated by polyglycylated forms of tubulin. Nevertheless we decided to investigate the modification of upheld, a homolog of troponin T, because this protein has an extended glutamate-rich C-terminal tail that could serve as a potential site of modification.

The proteins chosen for further analysis, RPT1, TCP1β, paramyosin, HSC70Cb, HSP60B and troponin T were cloned into mammalian expression vectors bearing a C-terminal (or, in the case of troponin T, a N-terminal) EYFP-tag. Expression in HEK293 cells confirmed that proteins of the correct size were expressed as EYFP-fusion proteins.

Supplementary materials and methods:

Sequencing of human genomic DNA

Genomic DNA was purified from human blood or sperm using the REDExtract-N-Amp™ Tissue PCR kit (Sigma, USA). Each DNA was amplified with the primer pair

hTTLL10_seq_F1263 (5'-CATGCAGAAGAAGAGCCCTCTGTAC-3')

hTTLL10_seq_introRa (5'-CTGCCAAGTGGAGGATCTGAAAGG-3')

in two independent polymerase chain reactions (PCRs). The resulting PCR products of approximately 500 bp were purified and sequenced with both primers. No PCR-related mutation was detected.

Protein identification by mass spectrometry

Protein preparation for in gel digestion. The gel pieces were cut out from a Coomassie brilliant blue stained gel and successively washed with 50 µl of 25 mM NH_4HCO_3 and 50 µl of acetonitrile (three times), and dehydrated with 100 µl of acetonitrile before reduction in the presence of 10 mM DTT in 25 mM NH_4HCO_3 (1 h at 57°C) and alkylation in the presence of 55 mM iodoacetamide in 25 mM NH_4HCO_3. For tryptic digestion, the gel pieces were resuspended in 2 volumes of trypsin (12.5 ng/µl; V5111 Promega, USA) freshly diluted in 25 mM NH_4HCO_3 and incubated overnight at 37°C. The digested peptides were then extracted from the gel in a buffer containing 34.9% H_2O, 65% acetonitrile, and 0.1% HCOOH, and directly analyzed by nanoLC-MS/MS.

Chromatography conditions on NanoAcquity. The analysis was performed on a nanoACQUITY Ultra-Performance-LC (UPLC, Waters, Milford, USA). The samples were trapped on a 20x0.18 mm, 5 µm Symmetry C18 precolumn (Waters, Milford, USA), and the peptides were separated on a ACQUITY UPLC® BEH130 C18 column (Waters, Milford, USA), 75 µm x 200 mm, 1.7 µm particle size. The solvent system consisted of 0.1% formic acid in water (solvent A) and 0.1% formic acid in acetonitrile (solvent B). Trapping was performed during 3 min at 5 µl/min with 99% of solvent A and 1% of solvent B. Elution was performed at a flow rate of 400 nl/min, using 1-40% gradient (solvent B) over 35 min at 45°C followed by 65% (solvent B) over 5 min.

MS and MS/MS conditions on SYNAPT mass spectrometer. The MS and MS/MS analyzes were performed on the SYNAPT™ an hybrid quadrupole orthogonal acceleration time-of-flight tandem mass spectrometer (Waters, Milford, USA) equipped with a Z-spray ion source and a lock mass system. The system operates in positive mode and the capillary voltage was set at 3.5 KV and the cone voltage at 35 V. Mass calibration of the TOF was achieved using phosphoric acid (H_3PO_4) on the [50;2000] m/z range. Online correction of this calibration was performed with Glu-fibrino-peptide B as the lock-mass. The ion $(M+2H)^{2+}$ at m/z 785.8426 is used to calibrate MS data and the fragment ion $(M+H)^{+}$ at m/z 684.3469 is used to calibrate MS/MS data during the analysis.

For tandem MS experiments, the system was operated with automatic switching between MS and MS/MS modes (MS 0.5 s/scan on m/z range [250;1500] and MS/MS 0.7 s/scan on m/z range [50;2000]). The 3 most abundant peptides (intensity threshold 60 counts/s), preferably doubly and triply charged ions, were selected on each MS spectrum for further isolation and CID fragmentation with 2 energies set using collision energy profile. Fragmentation was performed using argon as the collision gas. The complete system was fully controlled by MassLynx 4.1 (SCN 566, Waters, Milford, USA). Raw data collected during nanoLC-MS/MS analyses were processed and converted with ProteinLynx Browser 2.3 (Waters, Milford, USA) into .pkl peak list format. Normal background substraction type was used for both MS and MS/MS with 5% threshold and polynomial correction of order 5, and deisotoping was performed.

Data analysis and protein identification. Mass data collected during LC-MS/MS analyses were processed using the software tool ProteinLynx Global Server (version 2.3; Waters, Milford, USA) converted into pkl files. The MS/MS data were analyzed using the MASCOT 2.2.0. algorithm (Matrix Science, UK) to search against a *Drosophila melanogaster* data base extracted from NCBInr (15th December 2008) concatenated with reversed copies of all sequences (182,083 entries). Spectra were searched with a mass tolerance of 30 ppm for MS and 0.05 Da for MS/MS data, allowing a maximum of one missed cleavage site by trypsin and with carbamidomethylation of cysteines and oxidation of methionines fixed as variable modifications. Protein identifications were validated when at least two peptides were identified with Mascot ion score greater than 35 for each MS/MS spectra.

For the estimation of the false positive rate in protein identification, a target-decoy database search was performed (Elias & Gygi, 2007). The false positive rate was close to 0.5%.

Criteria used for protein identifications followed the general guidelines for reporting proteomic experiments (MIAPE; http://www.psidev.info)

Supplementary references:

Elias, J.E., and Gygi, S.P. (2007) Target-decoy search strategy for increased confidence in large-scale protein identifications by mass spectrometry. Nat Methods ***4***, 207-214.

Zhong, L., and Belote, J.M. (2007). The testis-specific proteasome subunit Prosalpha6T of D. melanogaster is required for individualization and nuclear maturation during spermatogenesis. Development *134*, 3517-3525.